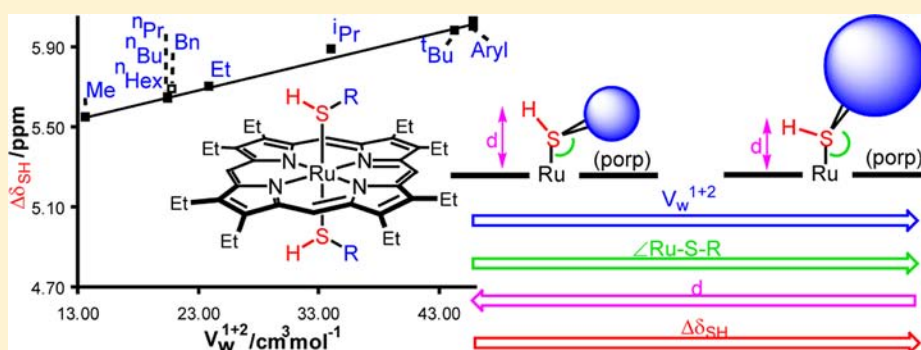


Molecular Recognition Using Ruthenium(II) Porphyrin Thiol Complexes as Probes

Júlio S. Rebouças^{*,†} and Brian R. James^{*,‡}[†]Departamento de Química, CCEN, Universidade Federal da Paraíba, João Pessoa, PB 58.051-900, Brazil[‡]Department of Chemistry, University of British Columbia, Vancouver, British Columbia V6T 1Z1, Canada

S Supporting Information



ABSTRACT: In situ ^1H NMR data are reported for 106 $\text{Ru}(\text{porp})(\text{RSH})_2$ species, where porp is the dianion of β -octaethylporphyrin (OEP), *meso*-tetraphenylporphyrin (TPP), and its para-substituted tetraphenyl analogues (T-*p*-XPP; X = OMe, Me, F, Cl, CO_2Me , CF_3), *meso*-tetrakis(3,5-dimethylphenyl)porphyrin (T-*m,m'*- Me_2PP), and *meso*-tetramesitylporphyrin (TMP), and R = Me, Et, ^nPr , ^iPr , ^nBu , ^iBu , ^nHex , Bn (benzyl), Ph, and *p*- MeOC_6H_4 . The upfield shifts in the SH resonances upon coordination of the thiol reflect changes in the porphyrin ring current and are analyzed using an empirical model that depicts quantitatively the nonbonding, electronic, and steric interactions between the thiol ligands, where steric factors dominate, and the porphyrin plane, where electronic factors dominate; such interactions are typically involved in small-molecule recognition within metalloporphyrin systems. Implications of the findings to hemithiolate proteins and surface coordination chemistry are also briefly presented.

1. INTRODUCTION

Heme-containing proteins and enzymes are ubiquitous in nature and are involved in diverse biological functions such as small-molecule transport, storage, and activation, electron transfer, and catalysis.^{1,2} Despite this wide range of biological activity, the majority of these heme proteins share the same (or closely related) prosthetic group, an iron complex derived from protoporphyrin IX; the biological function is, therefore, controlled largely by the apoprotein moiety, which ultimately dictates the reactivity of the heme group.^{2c,3} The high specificity/selectivity of the processes is generally mediated by a molecular recognition pattern between the protein (host) and substrate (guest). The mechanism underlying the protein recognition process, albeit complex, is usually ascribed to complementary geometric features in connection with covalent and/or noncovalent interactions (e.g., electrostatic, π - π stacking, etc.).³

The use of metalloporphyrins as molecular scaffolds for the development of biomimetic or bioinspired systems has been extensively explored.^{1a,g,2,4} Indeed, coordination chemists have made major advances in designing functionalized porphyrin architectures that mimic the polypeptide environment, allow for selective recognition of a variety of exogenous substrates, and

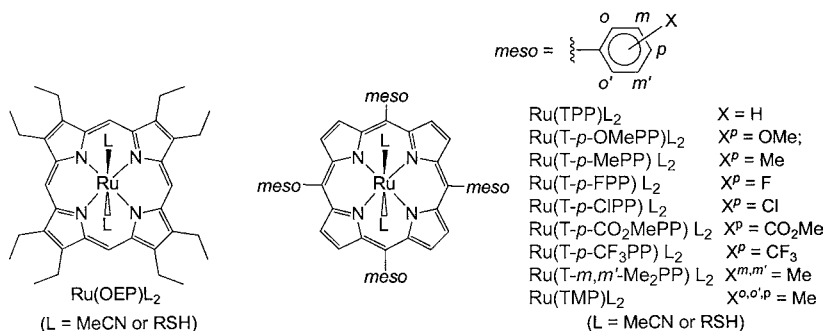
ultimately lead to functional biomimetic models.^{2,4} A natural extension of these studies resulted in the emergence of porphyrins as versatile building blocks for the preparation of chemical sensors and molecular switches because optical and redox properties of porphyrins are typically sensitive to interactions with the substrate and can be conveniently followed by spectroscopic and/or electrochemical means.^{4e,5}

The primary interaction mode between the metalloporphyrin and substrate is commonly an equilibrium, with the metal center and substrate being respectively the Lewis acid and base. This coordination is often fine-tuned via weaker interactions of the substrate with other chemical moieties within the porphyrin framework, a process usually referred to as multipoint molecular recognition.^{5g}

During the 1970s and early 1980s, efforts to model O_2 transport and storage by hemoglobin and myoglobin led to an understanding of the protein structure–function relationships in the binding of ligands to heme proteins.² Whereas unhindered iron(II) porphyrins such as $\text{Fe}(\text{TPP})$ ⁶ are irreversibly oxidized to μ -oxo species, the use of sterically

Received: November 2, 2012

Published: January 7, 2013

Chart 1. Ru(porp)(RSH)₂ Complexes

hindered porphyrin ligands (e.g., the so-called picket-fence, capped, and basket-handle porphyrins) prevented such oxidation and resulted in stabilization of the iron(II) state with reversible binding of O₂. Furthermore, selective recognition of O₂ versus other small molecules such as CO and H₂O was achieved by designing superstructures with hydrophobic pockets (to disfavor H₂O coordination), hydrogen-bonding capabilities (to stabilize coordinated O₂ via multipoint molecular recognition), and structural constraints (to explore differences between the coordination mode of O₂ and other small molecules). Similar effects on the coordination of other axial ligands were investigated by these biomimetic studies, and the importance of geometrical and functional complementarity between the porphyrin ligand pocket cavity and the substrate (guest) is now well documented;⁷ indeed, the shape-selective discrimination of small molecules imposed by sterically restrictive binding pockets within synthetic metalloporphyrins can sometimes surpass that observed in biological systems.^{7e}

Since the mid-1980s, the principles of small-molecule recognition have been studied upon modeling cytochrome P450⁴ and shape-selective, catalytic oxidation has been achieved via the use of superstructured metalloporphyrins^{4d,e} that incorporate dendrimers,⁸ cyclodextrin,⁹ and lipid bilayers;¹⁰ the reactivity is dictated by the complementary geometry of the substrate and catalyst. A remarkable example is the selective hydroxylation of inactive C–H bonds in steroid substrates containing also double bonds and secondary carbinol groups; the geometry prevents olefin epoxidation and oxidation of the alcohol functions, while exposing the saturated C–H bonds to the catalyst active site.⁹ The incorporation of chirality into a metalloporphyrin allows for asymmetric catalysis and generation of optically active sensors.^{4d–f,11} The emphasis has been on ruthenium porphyrins, which execute chiral recognition of substrates such as phosphines, alcohols, amino esters, and isocyanides^{4f} and carry out asymmetric oxidations, cyclopropanations, and carbene insertions.^{4f,g}

Although interactions of the substrate with an appended moiety or a sterically restricted binding site have been widely studied, the determinants of axial-ligand recognition imposed by the metalloporphyrin plane have received relatively little attention. Data on the coordination of pyridines and imidazoles¹² show that this is controlled by the basicity of the N atom, unless steric effects dominate as in 2- or 2,6-substituted pyridines or 2- or 2,4-substituted imidazoles,^{12c–i} which result from nonbonding interactions between the covalently bonded N-atom base and the relatively rigid porphyrin plane.¹² Such interactions have profound effects on the reactivity of the metal center.^{2d,12c,d,g–i}

We reported recently on 14 Ru(porp)(RSH)₂ complexes, where porp is the dianion of *meso*-tetramesitylporphyrin (TMP) or *meso*-tetrakis(4-methylphenyl)porphyrin (T-*p*MePP) and RSH is an aliphatic or aromatic thiol;¹³ ¹H NMR data showed that the ring-current-shift shielding of the SH proton depends on both the thiol and porphyrin.¹³ In this current paper, this study is extended to include 106 Ru(porp)(RSH)₂ species and shows that the SH resonance data provide an excellent entry to investigate systematically the steric and electronic effects involved in molecule recognition within these systems. The empirical model proposed depicts quantitatively the nonbonding interactions between the axial thiol ligands and the porphyrin plane and leads to speculative comments on the potential relevance of the findings to hemithiolate proteins and surface coordination chemistry.

2. EXPERIMENTAL SECTION

2.1. General Procedures. All reactions and manipulations were carried out under strictly anaerobic conditions. Argon (Praxair, 99.996%) was passed through an active Ridox column (Fisher Scientific), and N₂ (Praxair, 99.995%) was dried with Drierite (W.A. Hammond Co.). MeCN (Fisher Scientific, HPLC grade) was stored over activated molecular sieves (4 Å); C₆H₆ (Fisher Scientific) was treated with Na/benzoquinone, distilled under N₂, and used immediately. C₆D₆ was used as received from Cambridge Isotope Laboratories, Inc. Other solvents were of reagent grade purchased from Fisher Scientific or Aldrich Chemical Co. and before use were deoxygenated by purging with argon. Suba-seal and rubber septa were thoroughly washed with CH₂Cl₂ and dried at 40 °C prior to use. The free-base porphyrins H₂(porp) (see Chart 1) were prepared by literature methods using acid-catalyzed condensation of the appropriate pyrrole and aldehyde,¹³ except for H₂(OEP), which was kindly donated by D. Dolphin.

The Ru(porp)(CO)(L) complexes (L = MeCN, H₂O) were synthesized from Ru₃(CO)₁₂ (porp = OEP, TMP, T-*p*-XPP; X = OMe, Me, F, Cl, CF₃, CN)^{13,14} or from [Ru(DMF)₆](OTf)₃ (porp = OEP, TPP, T-*p*-CO₂MePP, T-*m,m'*-Me₂PP);¹⁵ porp = dianion of the parent H₂(porp) (see Chart 1). Thiols were obtained from Aldrich Chemical Co. and were used as received.

¹H and ¹⁹F{¹H} NMR spectra were measured in C₆D₆ at room temperature (rt; ~295 K) on a Bruker AV300 or AV400 spectrometer (300.13 and 400.13 MHz for ¹H, respectively) and referenced to residual solvent protons of tetramethylsilane-free C₆D₆ (δ 7.15); s = singlet, d = doublet, t = triplet, q = quartet, and m = multiplet (*J* values are given in hertz).

Multivariate linear regression and statistical analyses (at the 95% confidence level) were performed with the software package *Minitab for Windows* (Minitab Inc., version 10.1).

Tables and figures deposited in the Supporting Information (SI) are labeled respectively Tables SI-1–SI-5 and Figures SI-1–SI-21.

2.2. Preparation of Ru(porp)(MeCN)₂. The TMP and T-*p*-MePP complexes were prepared as previously described.¹³ The T-*p*-XPP (X

= OMe, H, F, Cl, CO₂Me, CF₃, CN) T-*m,m'*-Me₂PP, and OEP compounds were prepared via photolysis of the corresponding Ru(porp)(CO)L precursor (L = MeCN, H₂O), following the procedure described for Ru(T-*p*-MePP)(MeCN)₂.¹³ ¹H NMR assignments were made by comparison with data for the corresponding Ru(carbonyl) precursors.^{13–15}

Ru(OEP)(MeCN)₂. ¹H NMR: δ 9.98 (s, 8H, *meso*-H), 4.02 (q, 16H, ³J_{HH} = 7.59, CH₂), 2.04 (t, 24H, ³J_{HH} = 7.59, CH₂CH₃), –2.57 (s, 6H, CH₃CN); the data agree with those reported.¹⁶

Ru(T-*p*-OMePP)(MeCN)₂. ¹H NMR: δ 9.05 (s, 8H, β-pyrrole), 8.46 (AA'BB', 8H, *o*-C₆H₄OMe), 4.26 (s, 12H, OCH₃), –2.13 (s, 6H, CH₃CN). The unobserved *m*-C₆H₄OMe resonance lies under the residual solvent signal.

Ru(TPP)(MeCN)₂. ¹H NMR: δ 8.89 (s, 8H, β-pyrrole), 8.51–8.48 (m, 8H, *o*-C₆H₅), 7.53–7.40 (m, 12H, *m*- and *p*-C₆H₅), –2.15 (s, 6H, CH₃CN).

Ru(T-*p*-FPP)(MeCN)₂. ¹H{¹⁹F} NMR: δ 8.80 (s, 8H, β-pyrrole), 8.26 (AA'BB', 8H, *o*-C₆H₄F), 7.12 (AA'BB', 8H, *m*-C₆H₄F), –2.10 (s, 6H, CH₃CN). ¹⁹F{¹H} NMR: δ –39.0 (s).

Ru(T-*p*-ClPP)(MeCN)₂. ¹H NMR: δ 8.77 (s, 8H, β-pyrrole), 8.19 (AA'BB', 8H, *o*-C₆H₄Cl), 7.41 (AA'BB', 8H, *m*-C₆H₄Cl), –2.12 (s, 6H, CH₃CN).

Ru(T-*p*-CO₂MePP)(MeCN)₂. ¹H NMR: δ 8.77 (s, 8H, β-pyrrole), 8.48–8.41 (m, 16H, *o*- and *m*-C₆H₄CO₂Me), 3.66 (s, 12H, CO₂CH₃), –2.07 (s, 6H, CH₃CN).

Ru(T-*p*-CF₃PP)(MeCN)₂. ¹H NMR: δ 8.66 (s, 8H, β-pyrrole), 8.33 (AA'BB', 8H, *o*-C₆H₄CF₃), 7.67 (AA'BB', 8H, *m*-C₆H₄CF₃), –2.09 (s, 6H, CH₃CN). ¹⁹F{¹H} NMR: δ 15.2 (s).

Ru(T-*p*-CNPP)(MeCN)₂. ¹H NMR: δ 8.58 (s, 8H, β-pyrrole), 8.08 (AA'BB', 8H, *o*-C₆H₄CN), 7.26 (AA'BB', 8H, *m*-C₆H₄CN), –2.09 (s, 6H, CH₃CN).

Ru(T-*m,m'*-Me₂PP)(MeCN)₂. ¹H NMR: δ 8.99 (s, 8H, β-pyrrole), 8.18 (s, 8H, *o*-C₆H₃Me₂), 2.42 (s, 24H, *m*-CH₃), –2.01 (s, 6H, CH₃CN). The unobserved *p*-C₆H₃Me₂ resonance lies under the residual solvent signal.

2.3. Preparation of Ru(porp)(RSH)₂. C₆D₆ solutions of Ru(porp)(MeCN)₂ were reacted in situ with RSH (RSH:Ru ~10) at rt exactly as described previously,^{13a} using gaseous or liquid RSH (R = Me, Et, ^{*n*}Pr, ^{*i*}Pr, ^{*n*}Bu, ^{*t*}Bu, ^{*n*}Hex, Bn, Ph, *p*-MeOC₆H₄) or solid RSH (R = *p*-MeC₆H₄, *p*-ClC₆H₄, *p*-BrC₆H₄); in all cases, the δ 0.59 6H resonance of free MeCN was observed. Chemical shifts are reported to the second decimal place, although analyses of different batches of Ru(porp)(RSH)₂ showed the reproducibility to within ±0.005 ppm. For the NMR data, C¹, C², C³, etc., of the axial ligands are defined as HS–C¹–C²–C³... or HS–C¹(C²–C³...)₂, etc. Typical ¹H NMR spectra are shown in Figure 1 of ref 13a.

2.3.1. Ru(OEP)(RSH)₂ (R = Me, Et, ^{*n*}Pr, ^{*i*}Pr, ^{*n*}Bu, ^{*t*}Bu, ^{*n*}Hex, Bn, Ph, *p*-MeOC₆H₄). Ru(OEP)(MeSH)₂. ¹H NMR: OEP, δ 9.75 (s, 8H, *meso*-H), 3.92 (q, 16H, ³J_{HH} = 7.60, CH₂), 1.92 (t, 24H, ³J_{HH} = 7.60, CH₃); MeSH, δ –3.00 (d, 6H, ³J_{HH} = 7.31, CH₃), –4.75 (q, 2H, ³J_{HH} = 7.31, SH).

Ru(OEP)(EtSH)₂. ¹H NMR: OEP, δ 9.78 (s, 8H, *meso*-H), 3.93 (q, 16H, ³J_{HH} = 7.54, CH₂), 1.94 (t, 24H, ³J_{HH} = 7.54, CH₃); EtSH, δ –1.84 (t, 6H, ³J_{HH} = 7.28, C²H₃), –2.55 to –2.65 (m, 4H, C¹H₂), –4.64 (t, 2H, ³J_{HH} = 7.25, SH).

Ru(OEP)(^{*n*}PrSH)₂. ¹H NMR: OEP, δ 9.77 (s, 8H, *meso*-H), 3.93 (q, 16H, ³J_{HH} = 7.63, CH₂), 1.91 (t, 24H, ³J_{HH} = 7.63, CH₃); ^{*n*}PrSH, δ –0.88 (t, 6H, ³J_{HH} = 7.30, C³H₃), –1.64 to –1.71 (m, 4H, C²H₂), –2.61 to –2.69 (m, 4H, C¹H₂), –4.62 (t, 2H, ³J_{HH} = 6.86, SH).

Ru(OEP)(^{*i*}PrSH)₂. ¹H NMR: OEP, δ 9.78 (s, 8H, *meso*-H), 3.93 (q, 16H, ³J_{HH} = 7.56, CH₂), 1.91 (t, 24H, ³J_{HH} = 7.56, CH₃); ^{*i*}PrSH, δ –1.77 (d, 12H, ³J_{HH} = 6.90, C²H₃), –2.20 to –2.35 (m, 2H, C¹H), –4.56 (d, 2H, ³J_{HH} = 3.02, SH).

Ru(OEP)(^{*n*}BuSH)₂. ¹H NMR: OEP, δ 9.77 (s, 8H, *meso*-H), 3.93 (q, 16H, ³J_{HH} = 7.56, CH₂), 1.94 (t, 24H, ³J_{HH} = 7.56, CH₃); ^{*n*}BuSH, δ –0.23 (t, 6H, ³J_{HH} = 7.32, C⁴H₃), –0.50 to –0.63 (m, 4H, C³H₂), –1.65 to –1.76 (m, 4H, C²H₂), –2.59 to –2.67 (m, 4H, C¹H₂), –4.61 (t, 2H, ³J_{HH} = 7.31, SH).

Ru(OEP)(^{*t*}BuSH)₂. ¹H NMR: OEP, δ 9.83 (s, 8H, *meso*-H), 3.95 (q, 16H, ³J_{HH} = 7.42, CH₂), 1.92 (t, 24H, ³J_{HH} = 7.42, CH₃); ^{*t*}BuSH, δ –1.88 (s, 18H, C²H₃), –4.37 (s, 2H, SH).

Ru(OEP)(^{*n*}HexSH)₂. ¹H NMR: OEP, δ 9.78 (s, 8H, *meso*-H), 3.93 (q, 16H, ³J_{HH} = 7.58, CH₂), 1.92 (t, 24H, ³J_{HH} = 7.58, CH₃); ^{*n*}HexSH, δ 0.56–0.47 (m, 10H, C⁶H₃ and C⁵H₂), 0.10–0.00 (m, 4H, C⁴H₂), –0.52 to –0.63 (m, 4H, C³H₂), –1.60 to –1.70 (m, 4H, C²H₂), –2.56 to –2.64 (m, 4H, C¹H₂), –4.59 (t, 2H, ³J_{HH} = 7.36, SH).

Ru(OEP)(BnSH)₂. ¹H NMR: OEP, δ 9.83 (s, 8H, *meso*-H), 3.93 (q, 16H, ³J_{HH} = 7.40, CH₂), 1.92 (t, 24H, ³J_{HH} = 7.40, CH₃); BnSH, δ 6.27–6.22 (m, 2H, *p*-Ph), 6.14–6.09 (m, 4H, *m*-Ph), 4.84–4.82 (m, 4H, *o*-Ph), –1.48 (d, 4H, ³J_{HH} = 7.41, CH₂), –4.30 (t, 2H, ³J_{HH} = 7.41, SH).

Ru(OEP)(PhSH)₂. ¹H NMR: OEP, δ 9.57 (s, 8H, *meso*-H), 3.88 (q, 16H, ³J_{HH} = 7.59, CH₂), 1.91 (t, 24H, ³J_{HH} = 7.59, CH₃); PhSH, δ 6.34–6.24 (m, 2H, *p*-Ph), 5.92–5.87 (m, 4H, *m*-Ph), 3.43–3.40 (m, 4H, *o*-Ph), –3.03 (s, 2H, SH).

Ru(OEP)(*p*-MeOC₆H₄SH)₂. ¹H NMR: OEP, δ 9.59 (s, 8H, *meso*-H), 3.90 (q, 16H, ³J_{HH} = 7.44, CH₂), 1.92 (t, 24H, ³J_{HH} = 7.44, CH₃); *p*-MeOC₆H₄SH, δ 5.59 (AA'XX', 4H, *m*-H), 3.40 (AA'XX', 4H, *o*-H), 3.01 (s, 6H, OCH₃), –2.98 (s, 2H, SH). The ortho and meta positions in *p*-MeOC₆H₄SH are relative to the SH.

2.3.2. Ru(T-*p*-OMePP)(RSH)₂ (R = Me, Et, ^{*n*}Pr, ^{*i*}Pr, ^{*n*}Bu, ^{*t*}Bu, ^{*n*}Hex, Bn, Ph, *p*-MeOC₆H₄). Ru(T-*p*-OMePP)(MeSH)₂. ¹H NMR: T-*p*-OMePP, δ 8.81 (s, 8H, β-pyrrole), 8.15 (AA'BB', 8H, *o*-C₆H₄OMe), 7.11 (AA'BB', 8H, *m*-C₆H₄OMe), 3.53 (s, 12H, OCH₃); MeSH, δ –2.54 (d, 6H, ³J_{HH} = 7.98, CH₃), –4.22 (q, 2H, ³J_{HH} = 7.98, SH).

Ru(T-*p*-OMePP)(EtSH)₂. ¹H NMR: T-*p*-OMePP, δ 8.85 (s, 8H, β-pyrrole), 8.19 (AA'BB', 8H, *o*-C₆H₄OMe), 7.12 (AA'BB', 8H, *m*-C₆H₄OMe), 3.52 (s, 12H, OCH₃); EtSH, δ –1.45 (t, 6H, ³J_{HH} = 7.42, C²H₃), –2.03 to –2.13 (m, 4H, C¹H₂), –4.06 (t, 2H, ³J_{HH} = 7.46, SH).

Ru(T-*p*-OMePP)(^{*n*}PrSH)₂. ¹H NMR: T-*p*-OMePP, δ 8.85 (s, 8H, β-pyrrole), 8.20 (AA'BB', 8H, *o*-C₆H₄OMe), 7.12 (AA'BB', 8H, *m*-C₆H₄OMe), 3.52 (s, 12H, OCH₃); ^{*n*}PrSH, δ –0.63 (t, 6H, ³J_{HH} = 7.31, C²H₃), –1.21 to –1.29 (m, 4H, C²H₂), –2.07 to –2.14 (m, 4H, C¹H₂), –4.05 (t, 2H, ³J_{HH} = 6.86, SH).

Ru(T-*p*-OMePP)(^{*i*}PrSH)₂. ¹H NMR: T-*p*-OMePP, δ 8.83 (s, 8H, β-pyrrole), 8.18 (AA'BB', 8H, *o*-C₆H₄OMe), 7.12 (AA'BB', 8H, *m*-C₆H₄OMe), 3.52 (s, 12H, OCH₃); ^{*i*}PrSH, δ –1.40 (d, 12H, ³J_{HH} = 6.61, C²H₃), –1.62 to –1.75 (m, 2H, C¹H), –3.99 (d, 2H, ³J_{HH} = 2.10, SH).

Ru(T-*p*-OMePP)(^{*n*}BuSH)₂. ¹H NMR: T-*p*-OMePP, δ 8.86 (s, 8H, β-pyrrole), 8.22 (AA'BB', 8H, *o*-C₆H₄OMe), 7.11 (AA'BB', 8H, *m*-C₆H₄OMe), 3.52 (s, 12H, OCH₃); ^{*n*}BuSH, δ –0.06 (t, 6H, ³J_{HH} = 7.38, C⁴H₃), –0.26 to –0.36 (m, 4H, C³H₂), –1.23 to –1.33 (m, 4H, C²H₂), –2.04 to –2.14 (m, 4H, C¹H₂), –4.03 (t, 2H, ³J_{HH} = 7.30, SH).

Ru(T-*p*-OMePP)(^{*t*}BuSH)₂. ¹H NMR: T-*p*-OMePP, δ 8.85 (s, 8H, β-pyrrole), 8.22 (AA'BB', 8H, *o*-C₆H₄OMe), 7.13 (AA'BB', 8H, *m*-C₆H₄OMe), 3.52 (s, 12H, OCH₃); ^{*t*}BuSH, δ –1.47 (s, 18H, C²H₃), –3.80 (s, 2H, SH).

Ru(T-*p*-OMePP)(^{*n*}HexSH)₂. ¹H NMR: T-*p*-OMePP, δ 8.86 (s, 8H, β-pyrrole), 8.23 (AA'BB', 8H, *o*-C₆H₄OMe), 7.13 (AA'BB', 8H, *m*-C₆H₄OMe), 3.51 (s, 12H, OCH₃); ^{*n*}HexSH, δ 0.60–0.51 (m, 10H, C⁶H₃ + C⁵H₂), 0.29–0.18 (m, 4H, C⁴H₂), –0.26 to –0.37 (m, 4H, C³H₂), –1.18 to –1.26 (m, 4H, C²H₂), –2.00 to –2.10 (m, 4H, C¹H₂), –4.01 (t, 2H, ¹³J_{HH} = 7.00, SH).

Ru(T-*p*-OMePP)(BnSH)₂. ¹H NMR: δ 16 (AA'BB', 8H, *o*-C₆H₄OMe), 3.52 (s, 12H, OCH₃); BnSH, 6.43–6.39 (m, 2H, *p*-Ph), 6.34–6.29 (m, 4H, *m*-Ph), 5.18–5.16 (m, 4H, *o*-Ph), –0.92 (d, 4H, ³J_{HH} = 7.44, CH₂), –3.71 (t, 2H, ³J_{HH} = 7.44, SH). The porp *m*-H signals are hidden by the residual solvent resonance.

Ru(T-*p*-OMePP)(PhSH)₂. ¹H NMR: T-*p*-OMePP, δ 8.76 (s, 8H, β-pyrrole), 8.10 (AA'BB', 8H, *o*-C₆H₄OMe), 3.57 (s, 12H, OCH₃); PhSH, δ 6.44–6.38 (m, 2H, *p*-Ph), 6.10–6.05 (m, 4H, *m*-Ph), 3.87–3.84 (m, 4H, *o*-Ph), –2.46 (s, 2H, SH). As above, the porp *m*-H signals are not seen.

Ru(T-*p*-OMePP)(*p*-MeOC₆H₄SH)₂. ¹H NMR: T-*p*-OMePP, δ 8.78 (s, 8H, β-pyrrole), 8.13 (AA'BB', 8H, *o*-C₆H₄OMe), 3.56 (s, 12H,

OCH₃); *p*-MeOC₆H₄SH, δ 5.75 (AA'XX', 4H, *m*-H), 3.84 (AA'XX', 4H, *o*-H), 3.02 (s, 6H, OCH₃), -2.45 (s, 2H, SH). As above, the porp *m*-H signals are not seen.

2.3.3. Ru(T-*p*-MePP)(RSH)₂ (R = Me, Et, ⁿPr, ⁱPr, ⁿBu, ^tBu, ⁿHex, Bn, Ph, *p*-MeOC₆H₄). The RSH complexes with R = Me, Et, ⁿPr, ⁱPr, ⁿBu, Bn, and Ph were described previously, including isolaton of the ^tBuSH complex, which confirmed the general formulation of the in situ species.^{13a}

Ru(T-*p*-MePP)(ⁿBuSH)₂. ¹H NMR: T-*p*-MePP, δ 8.81 (s, 8H, β -pyrrole), 8.21 (AA'BB', 8H, *o*-C₆H₄Me), 7.29 (AA'BB', 8H, *m*-C₆H₄Me), 2.39 (s, 12H, CH₃); ⁿBuSH, δ -0.07 (t, 6H, ³J_{HH} = 7.28, C⁴H₃), -0.28 to -0.40 (m, 4H, C³H₂), -1.25 to -1.35 (m, 4H, C²H₂), -2.06 to -2.14 (m, 4H, C¹H₂), -4.07 (t, 2H, ³J_{HH} = 6.99, SH).

Ru(T-*p*-MePP)(ⁿHexSH)₂. ¹H NMR: T-*p*-MePP, δ 8.81 (s, 8H, β -pyrrole), 8.21 (AA'BB', 8H, *o*-C₆H₄Me), 7.30 (AA'BB', 8H, *m*-C₆H₄Me), 2.39 (s, 12H, CH₃); ⁿHexSH, δ 0.68–0.59 (m, 4H, C⁵H₂), 0.56 (t, 6H, ³J_{HH} = 6.90, C⁶H₃), 0.28–0.18 (m, 4H, C⁴H₂), -0.28 to -0.38 (m, 4H, C³H₂), -1.18 to -1.28 (m, 4H, C²H₂), -2.03 to -2.11 (m, 4H, C¹H₂), -4.05 (t, 2H, ³J_{HH} = 7.30, SH).

Ru(T-*p*-MePP)(*p*-MeOC₆H₄SH)₂. ¹H NMR: T-*p*-MePP, δ 8.73 (s, 8H, β -pyrrole), 8.11 (AA'BB', 8H, *o*-C₆H₄Me), 7.34 (AA'BB', 8H, *m*-C₆H₄Me), 2.43 (s, 12H, CH₃); *p*-MeOC₆H₄SH, δ 5.73 (AA'XX', 4H, *m*-H), 3.82 (AA'XX', 4H, *o*-H), 3.05 (s, 6H, OCH₃), -2.49 (s, 2H, SH).

2.3.4. Ru(TPP)(RSH)₂ (R = Me, Et, ⁿPr, ⁱPr, ⁿBu, ^tBu, ⁿHex, Bn, Ph, *p*-MeOC₆H₄, *p*-MeC₆H₄, *p*-ClC₆H₄, *p*-BrC₆H₄). The ortho and meta positions in *p*-XC₆H₄SH are relative to the SH.

Ru(TPP)(MeSH)₂. ¹H NMR: TPP, δ 8.65 (s, 8H, β -pyrrole), 8.20–8.17 (m, 8H, *o*-Ph), 7.47–7.45 (m, 8H, *m*- + *p*-Ph); MeSH, δ -2.59 (d, 6H, ³J_{HH} = 7.51, CH₃), -4.32 (q, 2H, ³J_{HH} = 7.51, SH).

Ru(TPP)(EtSH)₂. ¹H NMR: TPP, δ 8.68 (s, 8H, β -pyrrole), 8.24–8.21 (m, 8H, *o*-Ph), 7.48–7.43 (m, 8H, *m*- + *p*-Ph); EtSH, δ -1.49 (t, 6H, ³J_{HH} = 7.41, C²H₃), -2.09 to -2.18 (m, 4H, C¹H₂), -4.15 (t, 2H, ³J_{HH} = 6.94, SH).

Ru(TPP)(ⁿPrSH)₂. ¹H NMR: TPP, δ 8.68 (s, 8H, β -pyrrole), 8.25–8.22 (m, 8H, *o*-Ph), 7.48–7.43 (m, 8H, *m*- + *p*-Ph); ⁿPrSH, δ -0.68 (t, 6H, ³J_{HH} = 7.32, C³H₃), -1.24 to -1.31 (m, 4H, C²H₂), -2.12 to -2.19 (m, 4H, C¹H₂), -4.14 (t, 2H, ³J_{HH} = 6.99, SH).

Ru(TPP)(ⁱPrSH)₂. ¹H NMR: TPP, δ 8.66 (s, 8H, β -pyrrole), 8.23–8.20 (m, 8H, *o*-Ph), 7.48–7.44 (m, 8H, *m*- + *p*-Ph); ⁱPrSH, δ -1.45 (d, 12H, ³J_{HH} = 6.63, C²H₃), -1.67 to -1.81 (m, 2H, C¹H), -4.07 (d, 2H, ³J_{HH} = 3.00, SH).

Ru(TPP)(ⁿBuSH)₂. ¹H NMR: TPP, δ 8.69 (s, 8H, β -pyrrole), 8.27–8.24 (m, 8H, *o*-Ph), 7.48–7.44 (m, 8H, *m*- + *p*-Ph); ⁿBuSH, δ -0.10 (t, 6H, ³J_{HH} = 7.28, C⁴H₃), -0.32 to -0.40 (m, 4H, C³H₂), -1.26 to -1.36 (m, 4H, C²H₂), -2.09 to -2.16 (m, 4H, C¹H₂), -4.12 (t, 2H, ³J_{HH} = 6.97, SH).

Ru(TPP)(^tBuSH)₂. ¹H NMR: TPP, δ 8.68 (s, 8H, β -pyrrole), 8.27–8.24 (m, 8H, *o*-Ph), 7.48–7.44 (m, 8H, *m*- + *p*-Ph); ^tBuSH, δ -1.52 (s, 18H, C²H₃), -3.89 (s, 2H, SH).

Ru(TPP)(ⁿHexSH)₂. ¹H NMR: TPP, δ 8.69 (s, 8H, β -pyrrole), 8.28–8.24 (m, 8H, *o*-Ph), 7.48–7.44 (m, 8H, *m*- + *p*-Ph); ⁿHexSH, δ 0.65–0.52 (m, 10H, C⁶H₃ + C⁵H₂), 0.26–0.16 (m, 4H, C⁴H₂), -0.29 to -0.39 (m, 4H, C³H₂), -1.19 to -1.29 (m, 4H, C²H₂), -2.06 to -2.13 (m, 4H, C¹H₂), -4.09 (t, 2H, ³J_{HH} = 7.21, SH).

Ru(TPP)(BnSH)₂. ¹H NMR: TPP, δ 8.71 (s, 8H, β -pyrrole), 8.21–8.18 (m, 8H, *o*-Ph), 7.46–7.41 (m, 8H, *m*- + *p*-Ph); BnSH, δ 6.43–6.38 (m, 2H, *p*-Ph), 6.32–6.27 (m, 4H, *m*-Ph), 5.15–5.13 (m, 4H, *o*-Ph), -0.98 (d, 4H, ³J_{HH} = 7.83, CH₂), -3.79 (t, 2H, ³J_{HH} = 7.83, SH).

Ru(TPP)(PhSH)₂. ¹H NMR: TPP, δ 8.61 (s, 8H, β -pyrrole), 8.15–8.12 (m, 8H, *o*-Ph), 7.53–7.48 (m, 8H, *m*- + *p*-Ph); PhSH, δ 6.41–6.35 (m, 2H, *p*-Ph), 6.06–6.00 (m, 4H, *m*-Ph), 3.82–3.79 (m, 4H, *o*-Ph), -2.56 (s, 2H, SH).

Ru(TPP)(*p*-MeOC₆H₄SH)₂. ¹H NMR: TPP, δ 8.62 (s, 8H, β -pyrrole), 8.18–8.15 (m, 8H, *o*-Ph), 7.52–7.48 (m, 8H, *m*- + *p*-Ph); *p*-MeOC₆H₄SH, δ 5.71 (AA'XX', 4H, *m*-H), 3.79 (AA'XX', 4H, *o*-H), 3.03 (s, 6H, OCH₃), -2.54 (s, 2H, SH).

Ru(TPP)(*p*-MeC₆H₄SH)₂. ¹H NMR: TPP, δ 8.61 (s, 8H, β -pyrrole), 8.13–8.11 (m, 8H, *o*-Ph), 7.53–7.48 (m, 8H, *m*- + *p*-Ph); *p*-

MeC₆H₄SH, δ 5.88 (AA'XX', 4H, *m*-H), 3.77 (AA'XX', 4H, *o*-H), 1.71 (s, 6H, CH₃), -2.57 (s, 2H, SH).

Ru(TPP)(*p*-ClC₆H₄SH)₂. ¹H NMR: TPP, δ 8.58 (s, 8H, β -pyrrole), 8.11–8.09 (m, 8H, *o*-Ph), 7.57–7.47 (m, 8H, *m*- + *p*-Ph); *p*-ClC₆H₄SH, δ 5.98 (AA'XX', 4H, *m*-H), 3.50 (AA'XX', 4H, *o*-H), -2.72 (s, 2H, SH).

Ru(TPP)(*p*-BrC₆H₄SH)₂. ¹H NMR: TPP, δ 8.58 (s, 8H, β -pyrrole), 8.11–8.09 (m, 8H, *o*-Ph), 7.57–7.47 (m, 8H, *m*- + *p*-Ph); *p*-BrC₆H₄SH, δ 5.98 (AA'XX', 4H, *m*-H), 3.49 (AA'XX', 4H, *o*-H), -2.72 (s, 2H, SH).

2.3.5. Ru(T-*p*-FPP)(RSH)₂ (R = Me, Et, ⁿPr, ⁱPr, ⁿBu, ^tBu, ⁿHex, Bn, Ph, *p*-MeOC₆H₄). The porp *m*-H signals are partially hidden by the residual solvent resonance.

Ru(T-*p*-FPP)(MeSH)₂. ¹H NMR: T-*p*-FPP, δ 8.56 (s, 8H, β -pyrrole), 7.94 (AA'BB', 8H, *o*-C₆H₄F); MeSH, δ -2.61 (d, 6H, ³J_{HH} = 7.82, CH₃), -4.36 (q, 2H, ³J_{HH} = 7.82, SH). ¹⁹F{¹H} NMR: δ -38.5 (s, *p*-F).

Ru(T-*p*-FPP)(EtSH)₂. ¹H NMR: T-*p*-FPP, δ 8.59 (s, 8H, β -pyrrole), 7.98 (AA'BB', 8H, *o*-C₆H₄F); EtSH, δ -1.49 (t, 6H, ³J_{HH} = 7.23, C²H₃), -2.12 to -2.23 (m, 4H, C¹H₂), -4.20 (t, 2H, ³J_{HH} = 6.97, SH). ¹⁹F{¹H} NMR: δ -38.5 (s, *p*-F).

Ru(T-*p*-FPP)(ⁿPrSH)₂. ¹H NMR: T-*p*-FPP, δ 8.59 (s, 8H, β -pyrrole), 8.00 (AA'BB', 8H, *o*-C₆H₄F); ⁿPrSH, δ -0.69 (t, 6H, ³J_{HH} = 7.32, C³H₃), -1.22 to -1.34 (m, 4H, C²H₂), -2.16 to -2.23 (m, 4H, C¹H₂), -4.19 (t, 2H, ³J_{HH} = 7.00, SH). ¹⁹F{¹H} NMR: δ -38.5 (s, *p*-F).

Ru(T-*p*-FPP)(ⁱPrSH)₂. ¹H NMR: T-*p*-FPP, δ 8.57 (s, 8H, β -pyrrole), 7.98 (AA'BB', 8H, *o*-C₆H₄F); ⁱPrSH, δ -1.46 (d, 12H, ³J_{HH} = 6.48, C²H₃), -1.74 to -1.84 (m, 2H, C¹H), -4.13 (d, 2H, ³J_{HH} = 2.75, SH). ¹⁹F{¹H} NMR: δ -38.5 (s, *p*-F).

Ru(T-*p*-FPP)(ⁿBuSH)₂. ¹H NMR: T-*p*-FPP, δ 8.60 (s, 8H, β -pyrrole), 8.01 (AA'BB', 8H, *o*-C₆H₄F); ⁿBuSH, δ -0.11 (t, 6H, ³J_{HH} = 7.36, C⁴H₃), -0.34 to -0.41 (m, 4H, C³H₂), -1.26 to -1.36 (m, 4H, C²H₂), -2.13 to -2.21 (m, 4H, C¹H₂), -4.17 (t, 2H, ³J_{HH} = 7.24, SH). ¹⁹F{¹H} NMR: δ -38.5 (s, *p*-F).

Ru(T-*p*-FPP)(^tBuSH)₂. ¹H NMR: T-*p*-FPP, δ 8.60 (s, 8H, β -pyrrole), 8.02 (AA'BB', 8H, *o*-C₆H₄F); ^tBuSH, δ -1.54 (s, 18H, C²H₃), -3.96 (s, 2H, SH). ¹⁹F{¹H} NMR: δ -38.5 (s, *p*-F).

Ru(T-*p*-FPP)(ⁿHexSH)₂. ¹H NMR: T-*p*-FPP, δ 8.61 (s, 8H, β -pyrrole), 8.03 (AA'BB', 8H, *o*-C₆H₄F); ⁿHexSH, δ 0.66–0.50 (m, 10H, C⁶H₃ + C⁵H₂), 0.24–0.14 (m, 4H, C⁴H₂), -0.31 to -0.41 (m, 4H, C³H₂), -1.19 to -1.29 (m, 4H, C²H₂), -2.09 to -2.18 (m, 4H, C¹H₂), -4.15 (t, 2H, ³J_{HH} = 6.86, SH). ¹⁹F{¹H} NMR: δ -38.4 (s, *p*-F).

Ru(T-*p*-FPP)(BnSH)₂. ¹H NMR: T-*p*-FPP, δ 8.63 (s, 8H, β -pyrrole), 7.95 (AA'BB', 8H, *o*-C₆H₄F); BnSH, δ 6.44–6.39 (m, 2H, *p*-Ph), 6.34–6.29 (m, 4H, *m*-Ph), 5.15–5.12 (m, 4H, *o*-Ph), -1.02 (d, 4H, ³J_{HH} = 7.43, CH₂), -3.84 (t, 2H, ³J_{HH} = 7.43, SH). ¹⁹F{¹H} NMR: δ -38.4 (s, *p*-F).

Ru(T-*p*-FPP)(PhSH)₂. ¹H NMR: T-*p*-FPP, δ 8.51 (s, 8H, β -pyrrole), 7.90 (AA'BB', 8H, *o*-C₆H₄F); PhSH, δ 6.40–6.35 (m, 2H, *p*-Ph), 6.03–5.98 (m, 4H, *m*-Ph), 3.76–3.73 (m, 4H, *o*-Ph), -2.60 (s, 2H, SH). ¹⁹F{¹H} NMR: δ -38.7 (s, *p*-F).

Ru(T-*p*-FPP)(*p*-MeOC₆H₄SH)₂. ¹H NMR: T-*p*-FPP, δ 8.53 (s, 8H, β -pyrrole), 7.93 (AA'BB', 8H, *o*-C₆H₄F); *p*-MeOC₆H₄SH, δ 5.70 (AA'XX', 4H, *m*-H), 3.74 (AA'XX', 4H, *o*-H), 2.98 (s, 6H, OCH₃), -2.58 (s, 2H, SH). ¹⁹F{¹H} NMR: δ -38.8 (s, *p*-F).

2.3.6. Ru(T-*p*-ClPP)(RSH)₂ (R = Me, Et, ⁿPr, ⁱPr, ⁿBu, ^tBu, ⁿHex, Bn, Ph, *p*-MeOC₆H₄). Ru(T-*p*-ClPP)(MeSH)₂. ¹H NMR: T-*p*-ClPP, δ 8.52 (s, 8H, β -pyrrole), 7.87 (AA'BB', 8H, *o*-C₆H₄Cl), 7.41 (AA'BB', 8H, *m*-C₆H₄Cl); MeSH, δ -2.66 (d, 6H, ³J_{HH} = 7.65, CH₃), 4.41 (q, 2H, ³J_{HH} = 7.65, SH).

Ru(T-*p*-ClPP)(EtSH)₂. ¹H NMR: T-*p*-ClPP, δ 8.55 (s, 8H, β -pyrrole), 7.92 (AA'BB', 8H, *o*-C₆H₄Cl), 7.41 (AA'BB', 8H, *m*-C₆H₄Cl); EtSH, δ -1.51 (t, 6H, ³J_{HH} = 7.25, C²H₃), -2.16 to -2.23 (m, 4H, C¹H₂), -4.23 (t, 2H, ³J_{HH} = 7.49, SH).

Ru(T-*p*-ClPP)(ⁿPrSH)₂. ¹H NMR: T-*p*-ClPP, δ 8.56 (s, 8H, β -pyrrole), 7.93 (AA'BB', 8H, *o*-C₆H₄Cl), 7.40 (AA'BB', 8H, *m*-C₆H₄Cl); ⁿPrSH, δ -0.70 (t, 6H, ³J_{HH} = 7.18, C³H₃), -1.27 to -1.35

(m, 4H, C²H₂), -2.17 to -2.27 (m, 4H, C¹H₂), -4.22 (t, 2H, ³J_{HH} = 6.91, SH).

Ru(T-*p*-ClIPP)(ⁱPrSH)₂. ¹H NMR: T-*p*-ClIPP, δ 8.54 (s, 8H, β-pyrrole), 7.92 (AA'BB', 8H, *o*-C₆H₄Cl), 7.42 (AA'BB', 8H, *m*-C₆H₄Cl); ⁱPrSH, δ -1.49 (d, 12H, ³J_{HH} = 6.53, C²H₃), -1.78 to -1.85 (m, 4H, C¹H₂), -4.17 (d, 2H, ³J_{HH} = 2.40, SH).

Ru(T-*p*-ClIPP)(ⁿBuSH)₂. ¹H NMR: T-*p*-ClIPP, δ 8.56 (s, 8H, β-pyrrole), 7.95 (AA'BB', 8H, *o*-C₆H₄Cl), 7.40 (AA'BB', 8H, *m*-C₆H₄Cl); ⁿBuSH, δ -0.11 (t, 6H, ³J_{HH} = 7.38, C⁴H₃), -0.35 to -0.42 (m, 4H, C³H₂), -1.29 to -1.39 (m, 4H, C²H₂), -2.14 to -2.24 (m, 4H, C¹H₂), -4.20 (t, 2H, ³J_{HH} = 6.64, SH).

Ru(T-*p*-ClIPP)(^tBuSH)₂. ¹H NMR: T-*p*-ClIPP, δ 8.56 (s, 8H, β-pyrrole), 7.96 (AA'BB', 8H, *o*-C₆H₄Cl), 7.43 (AA'BB', 8H, *m*-C₆H₄Cl); ^tBuSH, δ -1.56 (s, 18H, C²H₃), -4.00 (s, 2H, SH).

Ru(T-*p*-ClIPP)(ⁿHexSH)₂. ¹H NMR: T-*p*-ClIPP, δ 8.57 (s, 8H, β-pyrrole), 7.96 (AA'BB', 8H, *o*-C₆H₄Cl), 7.41 (AA'BB', 8H, *m*-C₆H₄Cl); ⁿHexSH, δ 0.64–0.49 (m, 10H, C⁶H₃ + C⁵H₂), 0.23–0.13 (m, 4H, C⁴H₂), -0.33 to -0.42 (m, 4H, C³H₂), -1.21 to -1.32 (m, 4H, C²H₂), -2.12 to -2.21 (m, 4H, C¹H₂), -4.18 (t, 2H, ³J_{HH} = 7.34, SH).

Ru(T-*p*-ClIPP)(BnSH)₂. ¹H NMR: T-*p*-ClIPP, δ 8.59 (s, 8H, β-pyrrole), 7.88 (AA'BB', 8H, *o*-C₆H₄Cl), 7.38 (AA'BB', 8H, *m*-C₆H₄Cl); BnSH, δ 6.44–6.38 (m, 2H, *p*-Ph), 6.34–6.28 (m, 4H, *m*-Ph), 5.13–5.10 (m, 4H, *o*-Ph), -1.05 (d, 4H, ³J_{HH} = 7.55, CH₂), -3.88 (t, 2H, ³J_{HH} = 7.55, SH).

Ru(T-*p*-ClIPP)(PhSH)₂. ¹H NMR: T-*p*-ClIPP, δ 8.48 (s, 8H, β-pyrrole), 7.84 (AA'BB', 8H, *o*-C₆H₄Cl), 7.46 (AA'BB', 8H, *m*-C₆H₄Cl); PhSH, δ 6.42–6.33 (m, 2H, *p*-Ph), 6.05–5.97 (m, 4H, *m*-Ph), 3.72–3.70 (m, 4H, *o*-Ph), -2.65 (s, 2H, SH).

Ru(T-*p*-ClIPP)(*p*-MeOC₆H₄SH)₂. ¹H NMR: T-*p*-ClIPP, δ 8.50 (s, 8H, β-pyrrole), 7.87 (AA'BB', 8H, *o*-C₆H₄Cl), 7.47 (AA'BB', 8H, *m*-C₆H₄Cl); *p*-MeOC₆H₄SH, 5.70 (AA'XX', 4H, *m*-H), 3.72 (AA'XX', 4H, *o*-H), 2.97 (s, 6H, OCH₃), -2.62 (s, 2H, SH).

2.3.7. Ru(T-*p*-CO₂MePP)(RSH)₂ (R = Me, Et, ⁿPr, ⁱPr, ⁿBu, ^tBu, ⁿHex, Bn, Ph, *p*-MeOC₆H₄). Ru(T-*p*-CO₂MePP)(MeSH)₂. ¹H NMR: T-*p*-CO₂MePP, δ 8.52 (s, 8H, β-pyrrole), 8.45 (AA'BB', 8H, *o*-C₆H₄CO₂Me), 8.13 (AA'BB', 8H, *m*-C₆H₄CO₂Me), 3.68 (s, 12H, CO₂CH₃); MeSH, δ -2.63 (d, 6H, ³J_{HH} = 7.50, CH₃), -4.38 (q, 2H, ³J_{HH} = 7.50, SH).

Ru(T-*p*-CO₂MePP)(EtSH)₂. ¹H NMR: T-*p*-CO₂MePP, δ 8.56 (s, 8H, β-pyrrole), 8.45 (AA'BB', 8H, *o*-C₆H₄CO₂Me), 8.17 (AA'BB', 8H, *m*-C₆H₄CO₂Me), 3.67 (s, 12H, CO₂CH₃); EtSH, δ -1.49 (t, 6H, ³J_{HH} = 7.30, C²H₃), -2.12 to -2.21 (m, 4H, C¹H₂), -4.20 (t, 2H, ³J_{HH} = 7.14, SH).

Ru(T-*p*-CO₂MePP)(ⁿPrSH)₂. ¹H NMR: T-*p*-CO₂MePP, δ 8.57 (s, 8H, β-pyrrole), 8.44 (AA'BB', 8H, *o*-C₆H₄CO₂Me), 8.18 (AA'BB', 8H, *m*-C₆H₄CO₂Me), 3.67 (s, 12H, CO₂CH₃); ⁿPrSH, δ -0.69 (t, 6H, ³J_{HH} = 7.30, C³H₃), -1.24 to -1.34 (m, 4H, C²H₂), -2.14 to -2.22 (m, 4H, C¹H₂), -4.19 (t, 2H, ³J_{HH} = 7.15, SH).

Ru(T-*p*-CO₂MePP)(ⁱPrSH)₂. ¹H NMR: T-*p*-CO₂MePP, δ 8.55 (s, 8H, β-pyrrole), 8.45 (AA'BB', 8H, *o*-C₆H₄CO₂Me), 8.17 (AA'BB', 8H, *m*-C₆H₄CO₂Me), 3.66 (s, 12H, CO₂CH₃); ⁱPrSH, δ -1.47 (d, 12H, ³J_{HH} = 6.63, C²H₃), -1.73 to -1.81 (m, 4H, C¹H₂), -4.13 (d, 2H, ³J_{HH} = 2.80, SH).

Ru(T-*p*-CO₂MePP)(ⁿBuSH)₂. ¹H NMR: T-*p*-CO₂MePP, δ 8.57 (s, 8H, β-pyrrole), 8.44 (AA'BB', 8H, *o*-C₆H₄CO₂Me), 8.20 (AA'BB', 8H, *m*-C₆H₄CO₂Me), 3.67 (s, 12H, CO₂CH₃); ⁿBuSH, δ -0.09 (t, 6H, ³J_{HH} = 7.30, C⁴H₃), -0.31 to -0.43 (m, 4H, C³H₂), -1.26 to -1.36 (m, 4H, C²H₂), -2.11 to -2.19 (m, 4H, C¹H₂), -4.16 (t, 2H, ³J_{HH} = 7.11, SH).

Ru(T-*p*-CO₂MePP)(^tBuSH)₂. ¹H NMR: T-*p*-CO₂MePP, δ 8.58 (s, 8H, β-pyrrole), 8.47 (AA'BB', 8H, *o*-C₆H₄CO₂Me), 8.22 (AA'BB', 8H, *m*-C₆H₄CO₂Me), 3.66 (s, 12H, CO₂CH₃); ^tBuSH, δ -1.55 (s, 18H, C²H₃), -3.95 (s, 2H, SH).

Ru(T-*p*-CO₂MePP)(ⁿHexSH)₂. ¹H NMR: T-*p*-CO₂MePP, δ 8.58 (s, 8H, β-pyrrole), 8.45 (AA'BB', 8H, *o*-C₆H₄CO₂Me), 8.21 (AA'BB', 8H, *m*-C₆H₄CO₂Me), 3.66 (s, 12H, CO₂CH₃); ⁿHexSH, δ 0.66–0.50 (m, 10H, C⁶H₃ + C⁵H₂), 0.25–0.15 (m, 4H, C⁴H₂), -0.30 to -0.41 (m, 4H, C³H₂), -1.19 to -1.29 (m, 4H, C²H₂), -2.08 to -2.16 (m, 4H, C¹H₂), -4.14 (t, 2H, ³J_{HH} = 7.20, SH).

Ru(T-*p*-CO₂MePP)(BnSH)₂. ¹H NMR: T-*p*-CO₂MePP, δ 8.59 (s, 8H, β-pyrrole), 8.42 (AA'BB', 8H, *o*-C₆H₄CO₂Me), 8.13 (AA'BB', 8H, *m*-C₆H₄CO₂Me), 3.67 (s, 12H, CO₂CH₃); BnSH, δ 6.45–6.40 (m, 2H, *p*-Ph), 6.34–6.29 (m, 4H, *m*-Ph), 5.15–5.12 (m, 4H, *o*-Ph), -0.99 (d, 4H, ³J_{HH} = 7.54, CH₂), -3.84 (t, 2H, ³J_{HH} = 7.54, SH).

Ru(T-*p*-CO₂MePP)(PhSH)₂. ¹H NMR: T-*p*-CO₂MePP, δ 8.50–8.48 (m, 16H, β-pyrrole + *o*-C₆H₄CO₂CH₃), 8.09 (AA'BB', 8H, *m*-C₆H₄CO₂CH₃), 3.69 (s, 12H, CO₂CH₃); PhSH, δ 6.41–6.36 (m, 2H, *p*-Ph), 6.04–5.99 (m, 4H, *m*-Ph), 3.77–3.74 (m, 4H, *o*-Ph), -2.61 (s, 2H, SH).

Ru(T-*p*-CO₂MePP)(*p*-MeOC₆H₄SH)₂. ¹H NMR: T-*p*-CO₂MePP, δ 8.50–8.48 (m, 16H, β-pyrrole + *o*-C₆H₄CO₂CH₃), 8.12 (AA'BB', 8H, *m*-C₆H₄CO₂CH₃), 3.68 (s, 12H, CO₂CH₃); *p*-MeOC₆H₄SH, δ 5.71 (AA'XX', 4H, *m*-H), 3.75 (AA'XX', 4H, *o*-H), 2.99 (s, 6H, OCH₃), -2.58 (s, 2H, SH).

2.3.8. Ru(T-*p*-CF₃PP)(RSH)₂ (R = Me, Et, ⁿPr, ⁱPr, ⁿBu, ^tBu, ⁿHex, Bn, Ph, *p*-MeOC₆H₄). Ru(T-*p*-CF₃PP)(MeSH)₂. ¹H NMR: T-*p*-CF₃PP, δ 8.41 (s, 8H, β-pyrrole), 8.02 (AA'BB', 8H, *o*-C₆H₄CF₃), 7.67 (AA'BB', 8H, *m*-C₆H₄CF₃); MeSH, δ -2.63 (d, 6H, ³J_{HH} = 7.55, CH₃), -4.38 (q, 2H, ³J_{HH} = 7.55, SH). ¹⁹F{¹H} NMR: δ 15.1 (s, *p*-CF₃).

Ru(T-*p*-CF₃PP)(EtSH)₂. ¹H NMR: T-*p*-CF₃PP, δ 8.44 (s, 8H, β-pyrrole), 8.06 (AA'BB', 8H, *o*-C₆H₄CF₃), 7.66 (AA'BB', 8H, *m*-C₆H₄CF₃); EtSH, δ -1.46 (t, 6H, ³J_{HH} = 7.47, C²H₃), -2.13 to -2.22 (m, 4H, C¹H₂), -4.20 (t, 2H, ³J_{HH} = 7.15, SH). ¹⁹F{¹H} NMR: δ 15.1 (s, *p*-CF₃).

Ru(T-*p*-CF₃PP)(ⁿPrSH)₂. ¹H NMR: T-*p*-CF₃PP, δ 8.45 (s, 8H, β-pyrrole), 8.07 (AA'BB', 8H, *o*-C₆H₄CF₃), 7.65 (AA'BB', 8H, *m*-C₆H₄CF₃); ⁿPrSH, δ -0.65 (t, 6H, ³J_{HH} = 7.31, C³H₃), -1.21 to -1.33 (m, 4H, C²H₂), -2.17 to -2.24 (m, 4H, C¹H₂), -4.19 (t, 2H, ³J_{HH} = 6.91, SH). ¹⁹F{¹H} NMR: δ 15.1 (s, *p*-CF₃).

Ru(T-*p*-CF₃PP)(ⁱPrSH)₂. ¹H NMR: T-*p*-CF₃PP, δ 8.43 (s, 8H, β-pyrrole), 8.05 (AA'BB', 8H, *o*-C₆H₄CF₃), 7.67 (AA'BB', 8H, *m*-C₆H₄CF₃); ⁱPrSH, δ -1.44 (d, 12H, ³J_{HH} = 6.60, C²H₃), -1.74 to -1.83 (m, 2H, C¹H), -4.14 (d, 2H, ³J_{HH} = 2.53, SH). ¹⁹F{¹H} NMR: δ 15.1 (s, *p*-CF₃).

Ru(T-*p*-CF₃PP)(ⁿBuSH)₂. ¹H NMR: T-*p*-CF₃PP, δ 8.45 (s, 8H, β-pyrrole), 8.09 (AA'BB', 8H, *o*-C₆H₄CF₃), 7.65 (AA'BB', 8H, *m*-C₆H₄CF₃); ⁿBuSH, δ -0.07 (t, 6H, ³J_{HH} = 7.32, C⁴H₃), -0.28 to -0.40 (m, 4H, C³H₂), -1.24 to -1.35 (m, 4H, C²H₂), -2.14 to -2.22 (m, 4H, C¹H₂), -4.17 (t, 2H, ³J_{HH} = 7.31, SH). ¹⁹F{¹H} NMR: δ 15.1 (s, *p*-CF₃).

Ru(T-*p*-CF₃PP)(^tBuSH)₂. ¹H NMR: T-*p*-CF₃PP, δ 8.46 (s, 8H, β-pyrrole), 8.10 (AA'BB', 8H, *o*-C₆H₄CF₃), 7.68 (AA'BB', 8H, *m*-C₆H₄CF₃); ^tBuSH, δ -1.52 (s, 18H, C²H₃), -3.96 (s, 2H, SH). ¹⁹F{¹H} NMR: δ 15.1 (s, *p*-CF₃).

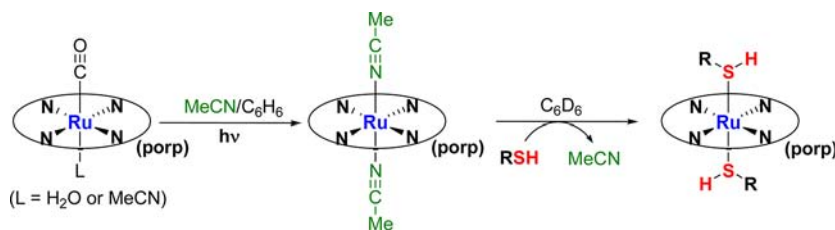
Ru(T-*p*-CF₃PP)(ⁿHexSH)₂. ¹H NMR: T-*p*-CF₃PP, δ 8.46 (s, 8H, β-pyrrole), 8.11 (AA'BB', 8H, *o*-C₆H₄CF₃), 7.67 (AA'BB', 8H, *m*-C₆H₄CF₃); ⁿHexSH, δ 0.64–0.49 (m, 10H, C⁶H₃ + C⁵H₂), 0.26–0.16 (m, 4H, C⁴H₂), -0.28 to -0.38 (m, 4H, C³H₂), -1.17 to -1.27 (m, 4H, C²H₂), -2.11 to -2.19 (m, 4H, C¹H₂), -4.15 (t, 2H, ³J_{HH} = 7.18, SH). ¹⁹F{¹H} NMR: δ 15.1 (s, *p*-CF₃).

Ru(T-*p*-CF₃PP)(BnSH)₂. ¹H NMR: T-*p*-CF₃PP, δ 8.48 (s, 8H, β-pyrrole), 8.02 (AA'BB', 8H, *o*-C₆H₄CF₃), 7.63 (AA'BB', 8H, *m*-C₆H₄CF₃); BnSH, δ 6.48–6.43 (m, 2H, *p*-Ph), 6.38–6.33 (m, 4H, *m*-Ph), 5.15–5.13 (m, 4H, *o*-Ph), -1.02 (d, 4H, ³J_{HH} = 7.43, CH₂), -3.86 (t, 2H, ³J_{HH} = 7.43, SH). ¹⁹F{¹H} NMR: δ 15.1 (s, *p*-CF₃).

Ru(T-*p*-CF₃PP)(PhSH)₂. ¹H NMR: T-*p*-CF₃PP, δ 8.37 (s, 8H, β-pyrrole), 7.98 (AA'BB', 8H, *o*-C₆H₄CF₃), 7.48 (AA'BB', 8H, *m*-C₆H₄CF₃); PhSH, δ 6.45–6.40 (m, 2H, *p*-Ph), 6.08–6.03 (m, 4H, *m*-Ph), 3.76–3.73 (m, 4H, *o*-Ph), -2.63 (s, 2H, SH). ¹⁹F{¹H} NMR: δ 15.2 (s, *p*-CF₃).

Ru(T-*p*-CF₃PP)(*p*-MeOC₆H₄SH)₂. ¹H NMR: T-*p*-CF₃PP, δ 8.40 (s, 8H, β-pyrrole), 8.02 (AA'BB', 8H, *o*-C₆H₄CF₃), 7.73 (AA'BB', 8H, *m*-C₆H₄CF₃); *p*-MeOC₆H₄SH, δ 5.74 (AA'XX', 4H, *m*-H), 3.74 (AA'XX', 4H, *o*-H), 2.97 (s, 6H, OCH₃), -2.60 (s, 2H, SH). ¹⁹F{¹H} NMR: δ 15.2 (s, *p*-CF₃).

2.3.9. Ru(T-*p*-CNPP)(RSH)₂ (R = Me, Et, ⁿPr, ⁱPr, ⁿBu, ^tBu, ⁿHex, Bn, Ph, *p*-MeOC₆H₄). The treatment of Ru(T-*p*-CNPP)(MeCN)₂ with the listed thiols in C₆D₆ yielded completely insoluble solids; precipitation

Scheme 1. Synthesis of the Ru(porp)(RSH)₂ Species

of the product was accompanied by the disappearance of the ¹H NMR signals of the reactant porphyrin and generation of a 6-proton resonance for free MeCN. Recovery and characterization of the solids were not attempted.

2.3.10. Ru(T-*m,m'*-Me₂PP)(RSH)₂ (R = Me, Et, ⁿPr, ⁱPr, ⁿBu, ^tBu, ⁿHex, Bn, Ph, *p*-MeOC₆H₄). The porp *p*-H signals are hidden under the residual solvent resonance.

Ru(T-*m,m'*-Me₂PP)(MeSH)₂. ¹H NMR: T-*m,m'*-Me₂PP, δ 8.80 (s, 8H, β-pyrrole), 7.95 (s, 8H, *o*-C₆H₃Me₂), 2.38 (s, 12H, CH₃); MeSH, δ -2.50 (d, 6H, ³J_{HH} = 7.28, CH₃), -4.21 (q, 2H, ³J_{HH} = 7.28, SH).

Ru(T-*m,m'*-Me₂PP)(EtSH)₂. ¹H NMR: T-*m,m'*-Me₂PP, δ 8.83 (s, 8H, β-pyrrole), 7.99 (s, 8H, *o*-C₆H₃Me₂), 2.38 (s, 12H, CH₃); EtSH, δ -1.43 (t, 6H, ³J_{HH} = 7.43, C²H₃), -1.99 to -2.09 (m, 4H, C¹H₂), -4.04 (t, 2H, ³J_{HH} = 7.28, SH).

Ru(T-*m,m'*-Me₂PP)(ⁿPrSH)₂. ¹H NMR: T-*m,m'*-Me₂PP, δ 8.83 (s, 8H, β-pyrrole), 8.00 (s, 8H, *o*-C₆H₃Me₂), 2.38 (s, 12H, CH₃); ⁿPrSH, δ -0.64 (t, 6H, ³J_{HH} = 7.33, C³H₃), -1.14 to -1.27 (m, 4H, C²H₂), -2.02 to -2.09 (m, 4H, C¹H₂), -4.03 (t, 2H, ³J_{HH} = 7.15, SH).

Ru(T-*m,m'*-Me₂PP)(^tPrSH)₂. ¹H NMR: T-*m,m'*-Me₂PP, δ 8.82 (s, 8H, β-pyrrole), 7.99 (s, 8H, *o*-C₆H₃Me₂), 2.38 (s, 12H, CH₃); ^tPrSH, δ -1.39 (d, 12H, ³J_{HH} = 6.60, C²H₃), -1.58 to -1.68 (m, 2H, C¹H), -3.95 (d, 2H, ³J_{HH} = 2.55, SH).

Ru(T-*m,m'*-Me₂PP)(ⁿBuSH)₂. ¹H NMR: T-*m,m'*-Me₂PP, δ 8.83 (s, 8H, β-pyrrole), 8.00 (s, 8H, *o*-C₆H₃Me₂), 2.39 (s, 12H, CH₃); ⁿBuSH, δ -0.07 (t, 6H, ³J_{HH} = 7.38, C⁴H₃), -0.26 to -0.38 (m, 4H, C³H₂), -1.19 to -1.29 (m, 4H, C²H₂), -2.00 to -2.07 (m, 4H, C¹H₂), -4.01 (t, 2H, ³J_{HH} = 7.15, SH).

Ru(T-*m,m'*-Me₂PP)(^tBuSH)₂. ¹H NMR: T-*m,m'*-Me₂PP, δ 8.84 (s, 8H, β-pyrrole), 8.03 (s, 8H, *o*-C₆H₃Me₂), 2.39 (s, 12H, CH₃); ^tBuSH, δ -1.45 (s, 18H, C²H₃), -3.79 (s, 2H, SH).

Ru(T-*m,m'*-Me₂PP)(ⁿHexSH)₂. ¹H NMR: T-*m,m'*-Me₂PP, δ 8.83 (s, 8H, β-pyrrole), 8.00 (s, 8H, *o*-C₆H₃Me₂), 2.39 (s, 12H, CH₃); ⁿHexSH, δ 0.67–0.51 (m, 10H, C⁶H₃ + C⁵H₂), 0.26–0.18 (m, 4H, C⁴H₂), -0.25 to -0.36 (m, 4H, C³H₂), -1.14 to -1.24 (m, 4H, C²H₂), -1.97 to -2.05 (m, 4H, C¹H₂), -3.99 (t, 2H, ³J_{HH} = 6.91, SH).

Ru(T-*m,m'*-Me₂PP)(BnSH)₂. ¹H NMR: T-*m,m'*-Me₂PP, δ 8.87 (s, 8H, β-pyrrole), 7.97 (s, 8H, *o*-C₆H₃Me₂), 2.36 (s, 12H, CH₃); BnSH, δ 6.42–6.37 (m, 2H, *p*-Ph), 6.31–6.26 (m, 4H, *m*-Ph), 5.21–5.18 (m, 4H, *o*-Ph), -0.87 (d, 4H, ³J_{HH} = 7.45, CH₂), -3.68 (t, 2H, ³J_{HH} = 7.45, SH).

Ru(T-*m,m'*-Me₂PP)(PhSH)₂. ¹H NMR: T-*m,m'*-Me₂PP, δ 8.74 (s, 8H, β-pyrrole), 7.88 (s, 8H, *o*-C₆H₃Me₂), 2.43 (s, 12H, CH₃); PhSH, δ 6.44–6.39 (m, 2H, *p*-Ph), 6.10–6.04 (m, 4H, *m*-Ph), 3.89–3.87 (m, 4H, *o*-Ph), -2.43 (s, 2H, SH).

Ru(T-*m,m'*-Me₂PP)(*p*-MeOC₆H₄SH)₂. ¹H NMR: T-*m,m'*-Me₂PP, δ 8.76 (s, 8H, β-pyrrole), 7.90 (s, 8H, *o*-C₆H₃Me₂), 2.44 (s, 12H, CH₃); *p*-MeOC₆H₄SH, δ 5.71 (AA'XX', 4H, *m*-H), 3.86 (AA'XX', 4H, *o*-H), 2.99 (s, 6H, OCH₃), -2.42 (s, 2H, SH).

2.3.11. Ru(TMP)(RSH)₂ (R = Me, Et, ⁿPr, ⁱPr, ⁿBu, ^tBu, ⁿHex, Bn, Ph, *p*-MeOC₆H₄, *p*-MeC₆H₄, *p*-ClC₆H₄, *p*-BrC₆H₄). The complexes with R = Me, Et, ⁿPr, ⁱPr, ^tBu, Bn, and Ph were described earlier.^{13a} The ortho and meta positions in the *p*-XC₆H₄SH fragment (X = OMe, Me, Cl, Br) are relative to the SH. The resonance of the *m*-mesityl protons lies under the residual solvent signal.

Ru(TMP)(ⁿBuSH)₂. ¹H NMR: TMP, δ 8.50 (s, 8H, β-pyrrole), 2.44 (s, 12H, *p*-CH₃), 2.11 (s, 24H, *o*-CH₃); ⁿBuSH, δ -0.13 (t, 6H, ³J_{HH} = 6.95, C⁴H₃), -0.21 to -0.29 (m, 4H, C³H₂), -0.71 to -0.81

(m, 4H, C²H₂), -1.83 to -1.90 (m, 4H, C¹H₂), -3.92 (t, 2H, ³J_{HH} = 8.36, SH).

Ru(TMP)(ⁿHexSH)₂. ¹H NMR: TMP, δ 8.51 (s, 8H, β-pyrrole), 2.43 (s, 12H, *p*-CH₃), 2.13 (s, 24H, *o*-CH₃); ⁿHexSH, δ 0.62–0.53 (m, 4H, C⁵H₂), 0.47 (t, 6H, ³J_{HH} = 6.89, C⁶H₃), 0.25–0.15 (m, 4H, C⁴H₂), -0.18 to -0.28 (m, 4H, C³H₂), -0.64 to -0.75 (m, 4H, C²H₂), -1.79 to -1.88 (m, 4H, C¹H₂), -3.89 (t, 2H, ³J_{HH} = 8.89, SH).

Ru(TMP)(*p*-MeOC₆H₄SH)₂. ¹H NMR: TMP, δ 8.51 (s, 8H, β-pyrrole), 2.44 (s, 12H, *p*-CH₃), 2.01 (s, 24H, *o*-CH₃); *p*-MeOC₆H₄SH, δ 5.64 (AA'XX', 4H, *m*-H), 4.15 (AA'XX', 4H, *o*-H), 2.85 (s, 6H, OCH₃), -2.03 (s, 2H, SH).

Ru(TMP)(*p*-MeC₆H₄SH)₂. ¹H NMR: TMP, δ 8.51 (s, 8H, β-pyrrole), 2.44 (s, 12H, *p*-CH₃), 1.98 (s, 24H, *o*-CH₃); *p*-MeC₆H₄SH, 5.79 (AA'XX', 4H, *m*-H), 4.10 (AA'XX', 4H, *o*-H), 1.50 (s, 6H, CH₃), -2.07 (s, 2H, SH).

Ru(TMP)(*p*-ClC₆H₄SH)₂. ¹H NMR: TMP, δ 8.46 (s, 8H, β-pyrrole), 2.44 (s, 12H, *p*-CH₃), 1.93 (s, 24H, *o*-CH₃); *p*-ClC₆H₄SH, 5.91 (AA'XX', 4H, *m*-H), 3.86 (AA'XX', 4H, *o*-H), -2.19 (s, 2H, SH).

Ru(TMP)(*p*-BrC₆H₄SH)₂. ¹H NMR: TMP, δ 8.46 (s, 8H, β-pyrrole), 2.44 (s, 12H, *p*-CH₃), 1.93 (s, 24H, *o*-CH₃); *p*-BrC₆H₄SH, 6.05 (AA'XX', 4H, *m*-H), 3.78 (AA'XX', 4H, *o*-H), -2.22 (s, 2H, SH).

3. RESULTS AND DISCUSSION

3.1. Thiol Complexes of Ruthenium(II) Porphyrins. We recently reported^{13a} on 14 Ru(porp)(RSH)₂ complexes (porp = T-*p*-MePP and TMP; RSH = aliphatic and aromatic thiols) and noted that the upfield ¹H NMR shifts of the SH proton depend on the thiol and porphyrin fragments. The use of further porphyrins and thiols has now provided such in situ ¹H data for 92 more species of this type, which allow for a systematic study of steric and electronic effects that govern small-molecule coordination to metalloporphyrins. The NMR data (see the Experimental Section) are entirely consistent with the Ru(porp)(RSH)₂ formulations (see Chart 1). The key resonance is that of the SH proton, which is the closest to the porphyrin ring current and the most upfield-shifted upon coordination of the thiol.^{13a} The systems are discussed in terms of Δδ_{SH}, which is the difference between the SH-proton shifts of the coordinated and free thiol; data for the latter are given in the SI (Table SI-1).

The RSH and porp reagents cover a wide range of steric and electronic features and include aliphatic thiols (R = Me, Et, ⁿPr, ⁿBu, ⁿHex, Bn, ⁱPrSH, ^tBuSH) and aromatic thiols with electron-donating and -withdrawing substituents [R = Ph, *p*-OMe(C₆H₄), *p*-Me(C₆H₄), *p*-Cl(C₆H₄), *p*-Br(C₆H₄); the porp anions were the β- and meso-substituted OEP and TPP, respectively, with the TPP derivatives having *o*-, *m*-, and *p*-phenyl moieties with electron-donating and -withdrawing substituents (Chart 1). Stronger σ-donor amine ligands (vs thiols)¹⁷ are commonly chosen for studies of molecular recognition,^{5c,f,g,12} but thiols have advantages: (i) the relatively stable Ru(porp)(RSH)₂ species are accessible via ligand exchange with Ru(porp)(MeCN)₂ (Scheme 1);^{13a} (ii) the SH proton is close to the coordination center and is not lost upon

Table 1. Ring-Current Shielding Shifts ($\Delta\delta_{\text{SH}}$) within the Ru(porp)(RSH)₂ Species^{a,b}

entry	R	porp									
		OEP	T-X-PP								TMP
			<i>p</i> -OMe	<i>p</i> -Me	<i>p</i> -H	<i>p</i> -F	<i>p</i> -Cl	<i>p</i> -CO ₂ Me	<i>p</i> -CF ₃	<i>m,m'</i> -Me ₂	
a	Me	5.55	5.02	5.07	5.12	5.16	5.21	5.18	5.18	5.01	4.84
b	Et	5.70	5.12	5.16	5.21	5.26	5.29	5.26	5.26	5.10	4.99
c	ⁿ Pr	5.64	5.07	5.11	5.16	5.21	5.24	5.21	5.21	5.05	4.95
d	ⁱ Pr	5.89	5.32	5.35	5.40	5.46	5.50	5.46	5.47	5.28	5.15
e	ⁿ Bu	5.65	5.07	5.11	5.16	5.21	5.24	5.20	5.21	5.05	4.96
f	^t Bu	5.98	5.41	5.45	5.50	5.57	5.61	5.56	5.54	5.40	5.31
g	ⁿ Hex	5.64	5.06	5.10	5.14	5.20	5.23	5.19	5.20	5.04	4.94
h	Bn	5.69	5.10	5.13	5.18	5.23	5.27	5.23	5.25	5.07	4.80
i	Ph	6.03	5.46	5.50	5.56	5.60	5.65	5.61	5.63	5.43	5.09
j	<i>p</i> -MeOC ₆ H ₄	6.00	5.47	5.51	5.56	5.60	5.64	5.60	5.62	5.44	5.05
k	<i>p</i> -MeC ₆ H ₄	–	–	–	–	5.58	–	–	–	–	5.08
l	<i>p</i> -ClC ₆ H ₄	–	–	–	–	5.56	–	–	–	–	5.03
m	<i>p</i> -BrC ₆ H ₄	–	–	–	–	5.54	–	–	–	–	5.04

^a δ values in ppm (C₆D₆, Ar); – implies complex not made. ^b $\Delta\delta_{\text{SH}} = \delta_{\text{SH}}(\text{free thiol}) - \delta_{\text{SH}}(\text{coordinated thiol})$; data for free thiols are given in Table SI-1 in the SI.

thiol coordination;^{13a} (iii) many aliphatic and aromatic thiols are commercially available; (iv) the SH group is relatively little involved in hydrogen-bonding interactions,¹⁸ in contrast to primary amines.^{13b,19}

Table 1 lists the $\Delta\delta_{\text{SH}}$ values for the Ru(porp)(RSH)₂ complexes: the experimental error in δ_{SH} is ± 0.005 ppm, and the uncertainty for the $\Delta\delta_{\text{SH}}$ values, determined by error propagation,²⁰ is about ± 0.008 ppm, which was conservatively rounded off to ± 0.01 ppm. The data were first analyzed by plotting $\Delta\delta_{\text{SH}}$ values for the Ru(porp)(RSH)₂ species against those for the corresponding Ru(TPP)(RSH)₂ species, with this porp system being chosen as the “standard”. The plots (Figures 1 and SI-1 in the SI) show excellent linearity for all porphyrins,

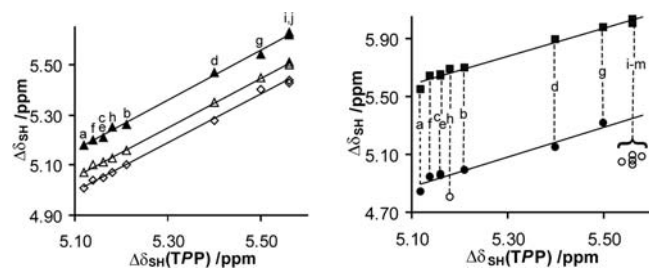


Figure 1. Plots of the $\Delta\delta_{\text{SH}}$ values for the Ru(porp)(RSH)₂ species versus the $\Delta\delta_{\text{SH}}$ values for Ru(TPP)(RSH)₂: (▲) T-*p*-CF₃PP; (△) T-*p*-MePP; (◇) T-*m,m'*-Me₂PP; (■) OEP; (●) TMP (excluding benzyl and aryl thiols); (○) TMP (benzyl and aryl thiols). Thiols are labeled (a–m), as in Table 1. Lines are fitted to the complete thiol series for each porphyrin (Table 2), except for TMP with the benzyl and aryl thiols (see the text). Other porphyrin plots are given in Figure SI-1 in the SI. Error bars in both *x* and *y* directions represented by the dimensions of the symbols.

except TMP with the Bn and aromatic thiols (Figure 1 and Table 2); if these thiols are excluded, the regression line follows that of the other porphyrins (Figure 1). This aspect of the Ru(TMP) systems is discussed in the next section. Of note, the slope values (b_1 or b_1' , Table 2) of the lines of Figures 1 and SI-1 in the SI are essentially unity, indicating that interactions between thiols and the ruthenium porphyrin moieties are governed by similar factors.

Table 2. Parameters of the Linear Regression of $\Delta\delta_{\text{SH}}$ Values for Ru(porp)(RSH)₂ Species against Those of the Ru(TPP)(RSH)₂ Species^a

porp	$y = b_1x + b_0$		$y = b_1'x$	
	b_1	b_0	R^2	b_1'
OEP	0.96 ± 0.05	0.7 ± 0.3	0.982	
T- <i>p</i> -OMePP	0.99 ± 0.02	<i>b</i>	0.998	0.9832 ± 0.0005
T- <i>p</i> -MePP	0.986 ± 0.008	<i>b</i>	0.9995	0.9906 ± 0.0003
T- <i>p</i> -FPP	1.00 ± 0.02	<i>b</i>	0.997	1.0096 ± 0.0006
T- <i>p</i> -ClPP	1.02 ± 0.02	<i>b</i>	0.998	1.0168 ± 0.0006
T- <i>p</i> -CO ₂ MePP	1.00 ± 0.02	<i>b</i>	0.998	1.0096 ± 0.0005
T- <i>p</i> -CF ₃ PP	1.01 ± 0.02	<i>b</i>	0.997	1.0109 ± 0.0006
T- <i>m,m'</i> -Me ₂ PP	0.97 ± 0.02	<i>b</i>	0.998	0.9789 ± 0.0005
TMP	0.5 ± 0.2	2.5 ± 0.5	0.484	
TMP ^c	1.0 ± 0.1	<i>b</i>	0.960	0.958 ± 0.003

^aCalculated using data in Table 1; see Figures 1 and SI-1 in the SI.

^bEssentially zero, not statistically significant (at the 95% confidence level), suggesting that the $y = b_1'x$ model is more appropriate.

^cExcluding benzyl and aryl thiols.

3.2. Electronic and Steric Effects of the Thiol Ligands.

The electronic effects of the thiol ligand appear not to influence their coordination. Plots of the $\Delta\delta_{\text{SH}}$ values versus thiol pK_a values (Table SI-2 in the SI) or Taft's polar substituent constants (σ^* ; Table SI-3 in the SI) were scattered for all of the ruthenium porphyrins (Figures SI-2–SI-7 in the SI); the $\Delta\delta_{\text{SH}}$ values are also insensitive to the Hammett σ_p constants for the phenyl substituents within the aromatic thiols (Figure 2; see Table 6). The data were then analyzed against Charton's steric parameter (ν ; Table SI-4 in the SI) and the revised Taft's steric constant (E_s' ; Table SI-5 in the SI) for the thiol R groups.²¹ There is no correlation with ν (Figures SI-8–SI-10 in the SI), but there is a poor correlation with E_s' (Figures SI-11–SI-13 in the SI), implying that steric factors may play a role. The regular Taft's steric constants (E_s) were not used because these correlate linearly with ν values.^{21c} A difficulty with steric parameters is that they are restricted to the same constraints of the systems from which they were derived: ν parameters are related to the radii of the substituent,^{21c} whereas E_s' values

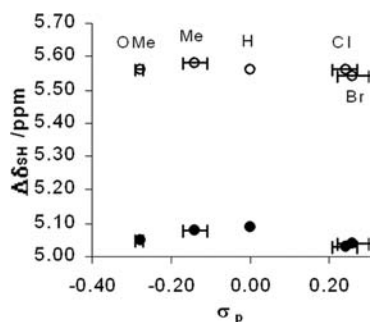


Figure 2. Plots of $\Delta\delta_{\text{SH}}$ values for $\text{Ru}(\text{TPP})(p\text{-XC}_6\text{H}_4\text{SH})_2$ (O) and $\text{Ru}(\text{TMP})(p\text{-XC}_6\text{H}_4\text{SH})_2$ (●) versus σ_p for the X substituent; see ref 25 for Br ($\sigma_p = 0.26 \pm 0.04$). Error bars in the y direction coincide with the symbol dimensions.

derive from kinetic data.^{21a} The data in Table 1 reveal that $\Delta\delta_{\text{SH}}$ depends qualitatively on the degree of substitution on C^1 (cf. entries a, h, b, d, and f) and C^2 (cf. entries b and c) of the thiols but is relatively insensitive to substitutions farther from the coordination site (cf. entries c, e, and g and also probably entries i–m). Crowding near the porphyrin plane thus seems to be controlling RSH coordination, and so the poor $\Delta\delta_{\text{SH}}$ versus E_s' correlation may result from steric effects near the reaction center influencing kinetics. Space constraints are not embedded in the ν parameters, which reflect the geometry of the whole substituent.

A purely geometric scale was thus devised to account for the effective bulkiness of the thiol ligands. The scale was constructed by combining the van der Waals volumes (V_w) of the groups assumed responsible for the crowdedness near the porphyrin plane: C^1 and C^2 in aliphatic thiols and Ph in aromatic thiols. These assumptions are considered chemically and geometrically reasonable because alkyl chains are flexible, and conformations in which a C atom such as C^3 or C^4 interacts with the porphyrin plane will be less significant. In contrast, the rigid Ph group contributes as a whole entity and will not deform to minimize interactions with the porphyrin plane; the contribution of remote para substituents to the effective bulkiness is regarded as irrelevant.

Table 3 lists the V_w values for some hydrocarbon groups,²² and Table 4 presents the “effective bulkiness” parameter

Table 3. van der Waals Volumes (V_w) for Hydrocarbon Groups^a

group	$V_w / \text{cm}^3 \text{mol}^{-1}$	group	$V_w / \text{cm}^3 \text{mol}^{-1}$
Alkanes ($X \neq \text{H}$)			
CX_4	3.33	CH_2X_2	10.23
CHX_3	6.78	CH_3X	13.67
Aromatics			
Ph	45.84	<i>ortho</i> -H	2.52
<i>ipso</i> -C	5.54		

^aData from ref 22.

(V_w^{1+2}) calculated from the V_w^1 and V_w^2 values for the C^1 and C^2 groups; for BnSH, the contribution of the Ph group (V_w^2) is less clear because CH_2 introduces some flexibility to the system. When the BnSH system is ignored, excellent linear correlations are seen between $\Delta\delta_{\text{SH}}$ and V_w^{1+2} (Figures 3 and SI-14 in the SI and Table 5). The $\Delta\delta_{\text{SH}}$ data for BnSH (Table 1), with the parameters from Table 5, imply that V_w^{1+2} is $\sim 21.8 \text{ cm}^3 \text{mol}^{-1}$, and because V_w^1 for CH_2 is 10.23, the V_w^2 value would be

Table 4. Combined van der Waals Volume for Thiol C^1 and C^2 Atoms^a

thiol	V_w^1	V_w^2	V_w^{1+2}
MeSH	13.67	0	13.67
EtSH	10.23	$1 \times 13.67 = 13.67$	23.90
ⁿ PrSH	10.23	$1 \times 10.23 = 10.23$	20.46
ⁱ PrSH	6.78	$2 \times 13.67 = 27.34$	34.12
ⁿ BuSH	10.23	$1 \times 10.23 = 10.23$	20.46
^t BuSH	3.33	$3 \times 13.67 = 41.01$	44.34
ⁿ HexSH	10.23	$1 \times 10.23 = 10.23$	20.46
BnSH	10.23	(10.58) ^{b,c}	(20.81) ^c
PhSH			45.84 ^{c,d}

^a V_w values are in $\text{cm}^3 \text{mol}^{-1}$. ^bEstimated for the partial Ph group [= *ipso*-C + ($2 \times$ *ortho*-H)]. ^cSee the text. ^dThe value of 45.84 was used also for $p\text{-XC}_6\text{H}_4\text{SH}$ ($X = \text{MeO}, \text{Me}, \text{Cl}, \text{Br}$).

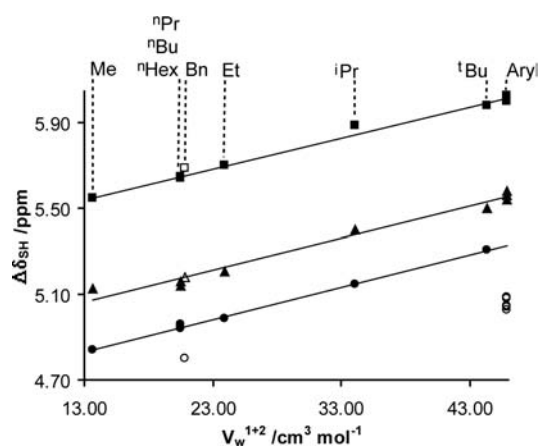


Figure 3. Plots of the $\Delta\delta_{\text{SH}}$ values for $\text{Ru}(\text{porp})(\text{RSH})_2$ species versus V_w^{1+2} values for the thiols: (■ and □) OEP; (▲ and Δ) TPP; (● and ○) TMP. Fitted lines (Table 5) exclude thiols marked with ○. Plots for other porphyrins are in Figure SI-14 in the SI. Error bars in the y direction represented by dimensions of the symbols.

Table 5. Linear Regression Parameters for Plots of $\Delta\delta_{\text{SH}}$ versus V_w^{1+2}

porp	slope/ppm mol cm^{-3}	y intercept/ppm	R^2
OEP	0.0145 ± 0.0006	5.35 ± 0.02	0.990
T- <i>p</i> -OMePP	0.0147 ± 0.0007	4.78 ± 0.03	0.984
T- <i>p</i> -MePP	0.0146 ± 0.0007	4.82 ± 0.03	0.983
TPP	0.0149 ± 0.0007	4.87 ± 0.03	0.982
T- <i>p</i> -FPP	0.0148 ± 0.0007	4.92 ± 0.02	0.987
T- <i>p</i> -ClPP	0.0151 ± 0.0009	4.95 ± 0.03	0.979
T- <i>p</i> -CO ₂ MePP	0.0147 ± 0.0009	4.92 ± 0.03	0.976
T- <i>p</i> -CF ₃ PP	0.015 ± 0.001	4.92 ± 0.04	0.970
T- <i>m,m'</i> -Me ₂ PP	0.0144 ± 0.0007	4.77 ± 0.02	0.987
TMP ^b	0.0152 ± 0.0004	4.636 ± 0.009	0.998

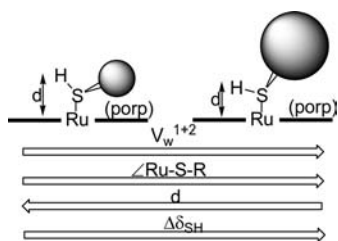
^aCalculated from data in Tables 1 and 4 (see Figures 3 and SI-14 in the SI), excluding data for BnSH (see the text). ^bAryl thiols not included.

~ 11.6 , which is much smaller than that of a Ph group. A calculated V_w^2 value (Tables 3 and 4), if considered as a combined contribution of the *ipso*-Ph C and both *o*-H atoms, is $10.58 \text{ cm}^3 \text{mol}^{-1}$, close to ~ 11.6 , and this seems a likely rationale because the position of the *ipso*-C is analogous to that of an aliphatic thiol C^2 and the *o*-H atoms are directed toward the porphyrin plane. As for Figure 1, the only points in Figures

3 and SI-14 in the SI that deviate from linearity are those for Ru(TMP)(RSH)₂ when R = Bn and aryl, implying that interactions between the porphyrin *o*-Me and thiol are likely relevant; for OEP and the meta- and para-substituted TPPs, the main interaction controlling thiol coordination appears to be between the R group and porphyrin plane. Of note, the linear regression slope for the Ru(TMP) systems, excluding the benzyl and aryl thiols, is comparable to those of the other ruthenium porphyrins (Table 5).

Because geometric parameters are able to describe $\Delta\delta_{\text{SH}}$ changes for a given Ru(porp) system, the increase in $\Delta\delta_{\text{SH}}$ with increasing V_w^{1+2} (Figure 3) is intuitively surprising in that a bulky thiol might be expected to lengthen the Ru–S distance, whereby the SH proton would be more distant from the porphyrin plane and π cloud. However, noting that there is minimal change in the geometry of free sulfur-containing ligands upon coordination at ruthenium porphyrin centers^{13a,23} and that the Ru–S bond lengths of Ru(OEP)[ⁿDecyl(Me)S]₂ and Ru(OEP)(Ph₂S)₂ are essentially the same^{23a} despite the increase in bulkiness upon going from the dialkyl to diaryl sulfide (cf. Table 4), the trend in Figure 3 can be rationalized. Assuming that the C1–S–H angle of the coordinated RSH does not change significantly from that of the free ligand, an increase in the Ru–S–C1 angle with a more bulky R group would translate into a decrease of the Ru–S–H angle, a shorter distance between the SH proton and the porphyrin plane (Scheme 2) and thus an increased $\Delta\delta_{\text{SH}}$ value (Figure 3).

Scheme 2. Effect of V_w^{1+2} on the Ru–S–R Angle and $\Delta\delta_{\text{SH}}$ Values



3.3. Electronic and Steric Effects of Porphyrin Substituents. The electronic effects were studied using Ru(porp)(RSH)₂ complexes with the para-substituted porphyrins (T-*p*-XPP; X = OMe, Me, H, F, Cl, CO₂Me, CF₃); the steric effects were similarly studied using OEP, T-*m,m'*-Me₂PP, and TMP. The electronic effects on $\Delta\delta_{\text{SH}}$ were analyzed using Hammett σ_p constants, derived from statistical calculations²⁴ and recommended by Exner.²⁵ The relevant values (Table 6)

Table 6. Hammett Constants for Porphyrin *meso*-Phenyl Substituents

substituent	σ_p or σ_m	porp	$\sum\sigma$
<i>p</i> -OMe	-0.28 ± 0.01	T- <i>p</i> -OMePP	-1.12 ± 0.04
<i>p</i> -Me	-0.14 ± 0.03	T- <i>p</i> -MePP	-0.56 ± 0.12
<i>p</i> -H	0	TPP	0
<i>p</i> -F	0.15 ± 0.06	T- <i>p</i> -FPP	0.60 ± 0.24
<i>p</i> -Cl	0.24 ± 0.03	T- <i>p</i> -ClPP	0.96 ± 0.12
<i>p</i> -CO ₂ Me	0.44 ± 0.09	T- <i>p</i> -CO ₂ MePP	1.76 ± 0.36
<i>p</i> -CF ₃	0.53 ± 0.11	T- <i>p</i> -CF ₃ PP	2.12 ± 0.44
<i>p</i> -CN	0.71 ± 0.08	T- <i>p</i> -CNPP	2.84 ± 0.32
<i>m</i> -Me	-0.06 ± 0.03	T- <i>m,m'</i> -Me ₂ PP	-0.48 ± 0.24

are in good agreement with other compilations;²⁶ of the 0.05–0.17 values suggested for F,^{24–28} the one listed is that recommended by Exner.²⁵ Table 6 also lists the sum of the Hammett constants ($\sum\sigma$) for some *meso*-tetraarylporphyrins. Unfortunately, $\Delta\delta_{\text{SH}}$ data for the T-*p*-CNPP species were not obtained because attempts to form the thiol complexes generated insoluble and, as yet, uncharacterized species.

The previous section shows that $\Delta\delta_{\text{SH}}$ values depend on the geometric parameter V_w^{1+2} for the RSH group and are independent of the electronic effects of the R group. However, the data of Figure 4 reveal a dependence on the $\sum\sigma_p$

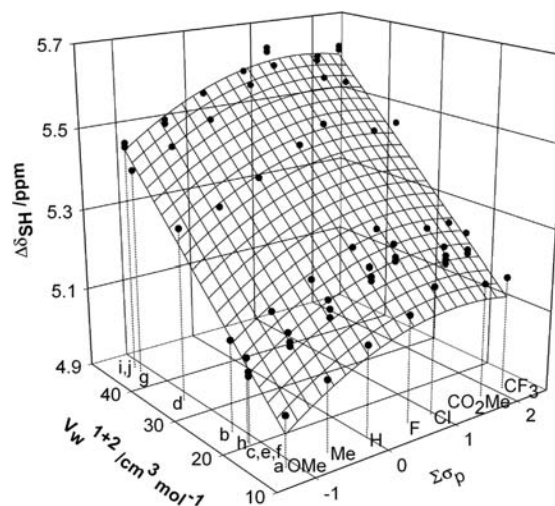


Figure 4. Thiol V_w^{1+2} and porphyrin $\sum\sigma_p$ parameters (eq 2 and Table 7) as descriptors of the $\Delta\delta_{\text{SH}}$ values for Ru(T-*p*-XPP)(RSH)₂ species (X = OMe, Me, H, F, Cl, CO₂Me, CF₃; RSH given as entries a–j in Table 1).

parameters of the porphyrin substituents, i.e., $\Delta\delta_{\text{SH}} = f(\sum\sigma_p, V_w^{1+2})$, and the curvature in the plots suggests that a second (or higher)-order model is required to describe the response surface.²⁹ Testing of a second-order model (eq 1) indicated that the $(V_w^{1+2})^2$ and $(\sum\sigma_p)(V_w^{1+2})$ terms were not needed, and the simplified model of eq 2 (validated in Figures SI-15 and SI-18 in the SI), with the parameters given in Table 7, generates the mesh shown in Figure 4. Neglect of the $(V_w^{1+2})^2$ term is consistent with the linear dependence on V_w^{1+2} demonstrated in section 3.2. Further, that $(\sum\sigma_p)(V_w^{1+2})$ is statistically nonsignificant (at the 95% confidence level) confirms that the $\Delta\delta_{\text{SH}}$ and V_w^{1+2} variables are independent (noninteracting) and thus can be analyzed individually; this is also consistent with the results of the previous section because

Table 7. Parameters for the $\Delta\delta_{\text{SH}}$, $\sum\sigma_p$, and V_w^{1+2} Terms in Equation 2 for the Ru(T-*p*-XPP)(RSH)₂ Species^a

parameter	eq 2 (X = OMe to CF ₃)	eq 3 (X = OMe, Me, H, F, Cl)	eq 4 (X = CO ₂ Me, CF ₃)
b_0	4.89 ± 0.01	4.873 ± 0.009	4.93 ± 0.02
b_1	0.074 ± 0.005	0.086 ± 0.005	^b
b_2	0.0148 ± 0.0003	0.0148 ± 0.0003	0.0148 ± 0.0006
b_{11}	-0.026 ± 0.004	^b	^b
R ²	0.977	0.985	0.974

^aLinear regression calculated using data from Tables 1, 4, and 6.

^bEssentially zero; not statistically significant (at the 95% confidence level).

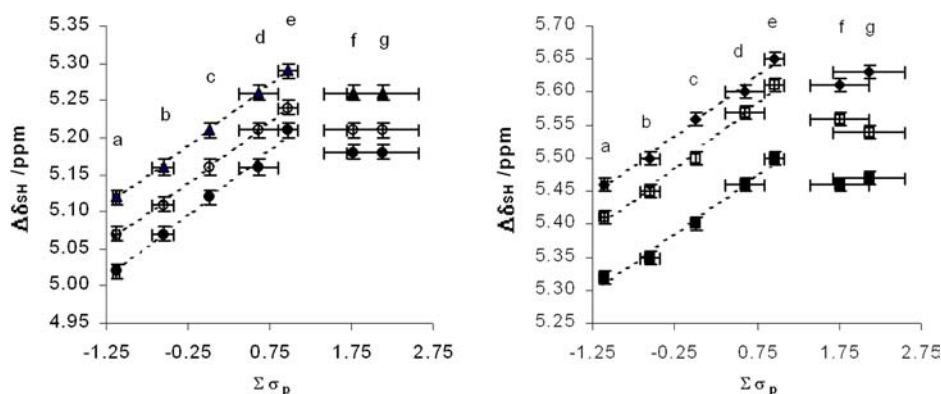


Figure 5. Plots of $\Delta\delta_{\text{SH}}$ versus $\sum\sigma_{\text{p}}$ for $\text{Ru}(\text{T-}p\text{-XPP})(\text{RSH})_2$; X = OMe (a), Me (b), H (c), F (d), Cl (e), CO_2Me (f), CF_3 (g). Left: RSH = (●) MeSH, (○) EtSH, and (▲) $^n\text{PrSH}$. Right: RSH = (■) $^i\text{PrSH}$, (□) $^t\text{BuSH}$, and (◆) PhSH. Table 8 gives parameters for the dotted lines. Plots for other thiols given in Figure SI-19 in the SI.

the slopes of the $\Delta\delta_{\text{SH}}$ versus V_{w}^{1+2} plots for the various porphyrins (Figures 3 and SI-14 in the SI) were similar to each other (Table 5) and the V_{w}^{1+2} coefficient (b_2) of eq 2 (Table 7).

$$\Delta\delta_{\text{SH}} = b_0 + b_1(\sum\sigma_{\text{p}}) + b_2(V_{\text{w}}^{1+2}) + b_{11}(\sum\sigma_{\text{p}})^2 + b_{22}(V_{\text{w}}^{1+2})^2 + b_{12}(\sum\sigma_{\text{p}})(V_{\text{w}}^{1+2}) \quad (1)$$

$$\Delta\delta_{\text{SH}} = b_0 + b_1(\sum\sigma_{\text{p}}) + b_2(V_{\text{w}}^{1+2}) + b_{11}(\sum\sigma_{\text{p}})^2 \quad (2)$$

The simplified model is mathematically and statistically sound, but the quadratic dependence of $\Delta\delta_{\text{SH}}$ on $\sum\sigma_{\text{p}}$ can only be rationalized if the “surface” is assumed to contain a discontinuity; this can be mathematically approximated if a continuous curvature along the $\sum\sigma_{\text{p}}$ axis is proposed. Because the dependence of $\Delta\delta_{\text{SH}}$ on $\sum\sigma_{\text{p}}$ and V_{w}^{1+2} may be treated independently, each thiol series (Table 1, entries a–j) was analyzed individually. Hammett plots (Figures 5 and SI-19 in the SI) show a linear dependence of $\Delta\delta_{\text{SH}}$ on $\sum\sigma_{\text{p}}$ for the $\text{Ru}(\text{T-}p\text{-XPP})(\text{RSH})_2$ species (X = OMe, Me, H, F, Cl; the “OMe–Cl” series), whereas the shifts are almost constant with the strongest electron-withdrawing groups (X = CO_2Me , CF_3). The parameters for the regression lines of the plots for the OMe–Cl series for each thiol are presented in Table 8; the fit to the experimental data is excellent, and the similar slopes indicate that a common mechanism governs the electronic substituent effect on $\Delta\delta_{\text{SH}}$ for this series. These plots suggest also that the “surface” described by eq 2 may be approximated

by a combination of independent planes: $\Delta\delta_{\text{SH}} = f(\sum\sigma_{\text{p}}, V_{\text{w}}^{1+2})$ for the OMe–Cl series (eq 3 and Table 7), and $\Delta\delta_{\text{SH}} = f(V_{\text{w}}^{1+2})$ for the X = CO_2Me and CF_3 systems (eq 4 and Table 7). Figure 6 illustrates the fitting of these planes to the

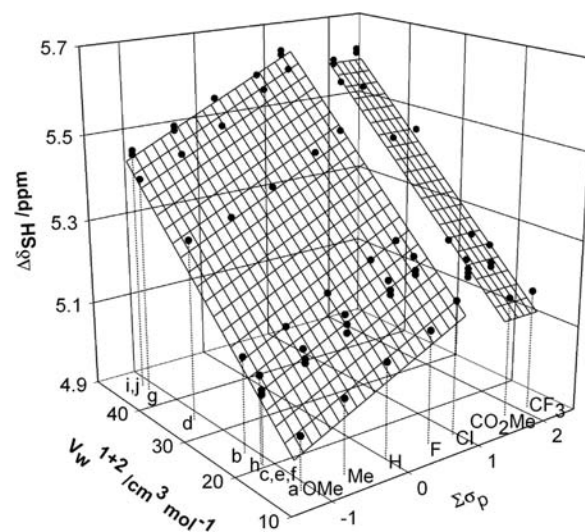


Figure 6. Thiol V_{w}^{1+2} and porphyrin $\sum\sigma_{\text{p}}$ parameters as descriptors of $\Delta\delta_{\text{SH}}$ values for $\text{Ru}(\text{T-}p\text{-XPP})(\text{RSH})_2$ species (X = OMe, Me, H, F, Cl, CO_2Me , CF_3 ; RSH given as entries a–j in Table 1). Planes described by eq 3 (X = OMe, Me, H, F, and Cl) and eq 4 (X = CO_2Me , CF_3) with parameters listed in Table 7.

Table 8. Parameters for the $\Delta\delta_{\text{SH}}$ versus $\sum\sigma_{\text{p}}$ Plots for the $\text{Ru}(\text{T-}p\text{-XPP})(\text{RSH})_2$ Species (X = OMe, Me, H, F, Cl)^a

thiol	slope/ppm	y intercept/ppm	R ²
MeSH	0.088 ± 0.005	5.118 ± 0.004	0.992
EtSH	0.083 ± 0.002	5.210 ± 0.002	0.999
$^n\text{PrSH}$	0.083 ± 0.002	5.160 ± 0.002	0.999
$^i\text{PrSH}$	0.088 ± 0.006	5.405 ± 0.005	0.986
$^t\text{BuSH}$	0.083 ± 0.002	5.160 ± 0.002	0.999
$^i\text{BuSH}$	0.097 ± 0.006	5.510 ± 0.004	0.991
$^n\text{HexSH}$	0.083 ± 0.004	5.148 ± 0.003	0.995
BnSH	0.082 ± 0.005	5.184 ± 0.004	0.989
PhSH	0.090 ± 0.006	5.557 ± 0.004	0.990
$p\text{-MeOC}_6\text{H}_4\text{SH}$	0.080 ± 0.003	5.558 ± 0.003	0.996

^aCalculated using data from Tables 1 and 6 (see Figures 5 and SI-19 in the SI).

experimental data. Statistical validation of the models described by eqs 3 and 4 is presented in Figures SI-16, SI-17, SI-20, and SI-21 in the SI.

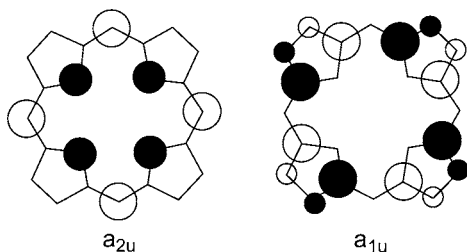
$$\Delta\delta_{\text{SH}} = b_0 + b_1(\sum\sigma_{\text{p}}) + b_2(V_{\text{w}}^{1+2}) \quad (3)$$

$$\Delta\delta_{\text{SH}} = b_0 + b_2(V_{\text{w}}^{1+2}) \quad (4)$$

The plots of Figures 5 and SI-19 in the SI can be rationalized. For the OMe–Cl systems, an increase in the Lewis acidity of the Ru center with increased electron-withdrawing character of the para substituents³⁰ might seem plausible because this would lead to a stronger Ru–thiol interaction, a shorter Ru–S bond, and thus higher $\Delta\delta_{\text{SH}}$ values. However, the Ru–S bond length varies little among various bis-sulfide, bis-disulfide, and bis-S-sulfoxide $\text{Ru}^{\text{II}}(\text{porp})$ complexes,^{13a,23} and this is even true for $\text{Ru}^{\text{II}}(\text{OEP})(^n\text{DecylSMe})_2$ and $[\text{Ru}^{\text{III}}(\text{OEP})(^n\text{DecylSMe})_2]\text{BF}_4$

which have different oxidation states.^{23a} A “saturation effect” whereby the Ru–S bond length becomes a constant minimal value is ruled out because the $\Delta\delta_{\text{SH}}$ values for Ru(T-*p*-CO₂MePP)(RSH)₂ and Ru(T-*p*-CF₃PP)(RSH)₂ are significantly smaller than those predicted using the linear relationship seen for the OMe–Cl series and are also consistently smaller than those observed for the Ru(T-*p*-ClPP)(RSH)₂ species. A reasonable explanation emerges, however, when the effects of peripheral substituents on the π -ring-current density are considered, with the more realistic concept that all of the Ru(T-*p*-XPP)(RSH)₂ species (X = OMe to CF₃) have essentially the same Ru–S bond length. Studies on porphyrin and metalloporphyrin ring-current effects are extensive^{31–33} (including some on ruthenium species),³¹ and Steiner et al. have shown theoretically that electron circulation maximizes within the *meso*-C atoms with contributions from the α -C and inner N atoms,^{33b,d} as exemplified in a magnesium porphyrin with a delocalized, 26-electron π system, where only the four associated with the porphyrin frontier orbitals contribute significantly to the ring current.^{33b} The classical Gouterman four-orbital model, showing the two nearly degenerate, energetically highest-filled, porphyrin-based molecular orbitals in *D*_{4h} symmetry (Chart 2),³⁴ remains relevant, and

Chart 2. *a*_{1u} and *a*_{2u} Porphyrin Frontier Orbitals in *D*_{4h} Symmetry



consequently fine tuning of the porphyrin π -electron flow may be achieved by modulation of the nearly degenerate *a*_{2u}/*a*_{1u} orbital structure, although this was not mentioned explicitly in the relevant literature.^{33b,d} The ruthenium porphyrin–thiol data provide strong experimental support for the model by Steiner et al. and also validate its underlying implication (see below). The data represent the first comprehensive attempt to use the model to interpret experimental observations on porphyrin ring currents.

Studies have shown that the *a*_{2u} and *a*_{1u} orbitals in π -cation radicals of ruthenium porphyrins are nearly degenerate and are in thermal equilibrium, with the overall orbital structure being an admixture of the two;³⁵ NMR analyses of Ru^{II}-TPP and -T-*p*-MePP complexes indicate that *a*_{2u} has slightly higher energy than *a*_{1u},^{35e} and the *a*_{1u}/*a*_{2u} configuration is sensitive to axial ligands (and temperature).^{35b–e} In [Fe^{III}(T-*p*-XPP)]⁺ systems, stronger electron-withdrawing para substituents result in a relative stabilization of the *a*_{2u} orbital,³⁶ which is consistent with significant atomic contributions of the *meso*-C atoms (Chart 2). If a similar situation exists in the Ru(T-*p*-XPP)(RSH)₂ systems, a change from a lower/higher *a*_{1u}/*a*_{2u} contribution for X = OMe, Me, H, F, and Cl to the reverse for X = CO₂Me and CF₃ could explain the plots of Figures 5 and SI-19 in the SI. The *a*_{1u}/*a*_{2u} orbital structure assigned to the OMe–Cl series is consistent with a dependence of $\Delta\delta_{\text{SH}}$ on $\sum\sigma_{\text{p}}$ and with the published data for Ru(TPP)(CO) and Ru(T-*p*-MePP)(CO).^{35e} If the *a*_{1u} orbital, which has nodes at the *meso* positions (Chart

2), is slightly higher in energy than *a*_{2u} for Ru(T-*p*-CO₂MePP)(RSH)₂ and Ru(T-*p*-CF₃PP)(RSH)₂, the ring current (and $\Delta\delta_{\text{SH}}$ values) would be expected to be essentially the same. Furthermore, a change in the frontier orbital from *a*_{2u} (X = Cl) to *a*_{1u} (X = CO₂Me, CF₃) would result in a significant modification of the ring electron pathway: the large contribution of the N atoms to *a*_{2u} translates into a higher current density near the core and close to the SH proton, whereas *a*_{1u} would be characterized by a more diffuse current predominately in the periphery of the ring. This is compatible with the fact that the $\Delta\delta_{\text{SH}}$ values for Ru(T-*p*-XPP)(RSH)₂ (X = CO₂Me, CF₃) are relatively independent of the electron-withdrawing ability of X and are consistently smaller than the values for the X = Cl species.

The porphyrin macrocycle can modify its σ - and π -bonding characteristics in response to the electronic effects of peripheral substituents and axial ligands, as exemplified in iron porphyrins by Mössbauer³⁷ and theoretical³⁸ data: the porphyrin ligand acts as an electron “sink” or “buffer” in order to maintain an approximately constant number of electrons around the metal center. Modifications of the electronic properties of the peripheral substituents of metalloporphyrins can also induce structural changes,³⁹ with an increase in the electron-withdrawing ability leading to a reduced size of the porphyrin core.^{39a,b,d,e} No such systematic studies have appeared on ruthenium porphyrins, but Spiro et al.^{39c,d,f} have shown that empirical correlations between resonance Raman and X-ray crystallographic parameters derived primarily from first-row metalloporphyrin data are extendable to the ruthenium complexes. Thus, if the “constant electron count” and “core size” properties are applicable, their combination could give rise to an intensification of the net ring-current density and provide a rationale for the $\Delta\delta_{\text{SH}}$ data for the OMe–Cl series. Although not mentioned in the original reference,^{39b} for solutions of the [Fe(T-*p*-XPP)]₂O complexes (X = OMe, H, CF₃), a resonance Raman porphyrin marker band correlates linearly (*R*² = 0.996) with $\sum\sigma_{\text{p}}$; the band frequency correlates inversely with the porphyrin core size, implying a linear constriction of the porphyrin core with an increase in the electron-withdrawing capability. Corresponding effects in our OMe–Cl species could well explain the linear $\Delta\delta_{\text{SH}}$ versus $\sum\sigma_{\text{p}}$ plots (Table 8).

Insight into how steric factors can effect the π -ring current and $\Delta\delta_{\text{SH}}$ is gleaned from data on the Ru(porp)(RSH)₂ complexes where porp = TMP, T-*m,m'*-Me₂PP, and OEP. As noted previously,^{13a} the Ru(TMP) moiety is less effective than Ru(T-*p*-MePP) in shielding the protons of thiols (and disulfides), and this is further established in this new work on considering that, compared to T-*p*-MePP, TMP has two additional *o*-Me substituents per *meso* group. Although separation of the steric and electronic effects associated with ortho substituents has been controversial,^{21d,40} the electronic contribution of a substituent in an ortho or para position is usually assumed to be about the same,^{21d,41} one study concluded that the electronic effect of an ortho substituent is ~80% of that of the same para substituent,⁴² implying a $\sigma_{\text{o}}^{\text{Me}}$ value of -0.11 ± 0.03 for Me (see Table 6), and thus a $\sum\sigma$ value for the TMP moiety of -1.44 ± 0.36 . Of note, porphyrin complexes are commonly noncoplanar even in solution at room temperature,^{14a} and the transmission of electronic effects are likely modulated by a rotational, conformation feature;⁴³ a hindered rotation of *meso*-aryl groups can occur irrespective of the presence of ortho substituents, as exemplified by the atropisomerism observed in meta-substituted ruthenium

porphyrins.⁴⁴ Assuming that the overall conformation of the *meso*-aryl and porphyrin rings does not change significantly among the *meso*-tetraarylporphyrins, their electronic effects should be about the same; i.e., the $\sum\sigma$ value for TMP is “on the same numerical scale” as the σ_p and σ_m values given in Table 6.

The lower $\Delta\delta_{\text{SH}}$ values for the Ru(TMP)(RSH)₂ species (Table 1; R = Me, Et, ⁿPr, ⁱPr, ⁿBu, ^tBu, ⁿHex) are linked with a more negative $\sum\sigma$ value relative to the analogous Ru(T-*p*-MePP)(RSH)₂ series (cf. Figure 7) and are qualitatively

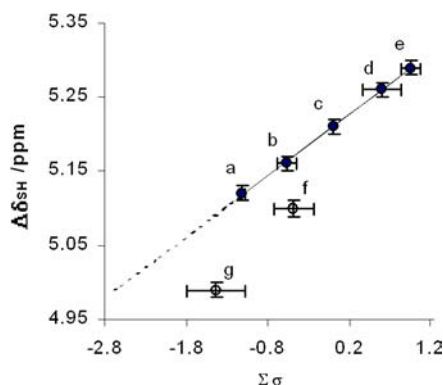


Figure 7. Plot of $\Delta\delta_{\text{SH}}$ versus $\sum\sigma_p$ for Ru(porp)(EtSH)₂ species: porp = T-*p*-OMePP (a), T-*p*-MePP (b), TPP (c), T-*p*-FPP (d), T-*p*-ClPP (e), T-*m,m'*-Me₂PP (f), and TMP (g); $\sum\sigma_p$ values given in Table 6. The fitted line excludes open symbols (parameters in Table 8). The dotted line is an extrapolation from the experimentally defined limits.

consistent with the data for the Ru(T-*p*-XPP)(RSH)₂ series. However, the $\Delta\delta_{\text{SH}}$ values for the TMP series are, on average, 0.10 ± 0.03 ppm lower than those estimated by the linear relationships devised for the corresponding OMe–Cl series, Ru(T-*p*-XPP)(RSH)₂ (R as above; Table 8); the benzyl and aromatic thiols are excluded because of their interactions with the *o*-Me groups in the Ru(TMP)(RSH)₂ complexes (section 3.2). The reason for the discrepancy between observed and estimated $\Delta\delta_{\text{SH}}$ values for Ru(TMP)(RSH)₂ complexes is believed to be a steric effect associated with the electronic effect of a mesityl substituent, which became evident during analysis of the data for Ru(T-*m,m'*-Me₂PP)(RSH)₂ species. An alternative explanation invokes a limit to which the electronic effect can modulate the porphyrin core size, with the TMP case being beyond such a limit. These explanations are discussed below.

While there is uncertainty associated with σ_o^{Me} (and thus $\sum\sigma$ for TMP), the σ_m^{Me} value is well established (Table 6).^{21d,24–26} On the basis of the $\sum\sigma$ values (Table 6), the $\Delta\delta_{\text{SH}}$ values for the Ru(T-*m,m'*-Me₂PP)(RSH)₂ and Ru(T-*p*-MePP)(RSH)₂ species should be similar, but those for the former are instead close to those of the Ru(T-*p*-OMePP)(RSH)₂ complexes (Table 1 and Figure 7), which have more negative $\sum\sigma$ values than those associated with the T-*m,m'*-Me₂P moiety (Table 6). In fact, all Ru(T-*m,m'*-Me₂PP)(RSH)₂ and Ru(TMP)(RSH)₂ complexes have lower $\Delta\delta_{\text{SH}}$ values than those estimated from the linear relationships devised for the OMe–Cl series, Ru(T-*p*-XPP)(RSH)₂ (Table 8); Figure 7 shows the deviations in the R = Et systems, and similar trends exist for other thiol species. Whereas the $\sum\sigma$ value of -1.44 ± 0.36 for TMP (see above) extrapolates the range of values used in the linear relationships in the OMe–Cl series, this is not so for Ru(T-*m,m'*-Me₂PP)(RSH)₂, and so a “saturation electronic effect” for this series is ruled out. Moreover, in order for the Ru(T-*m,m'*-

Me₂PP)(RSH)₂ data to fit the OMe–Cl series trend line, the $\sum\sigma$ value for the porp moiety would have to be about -1.34 , implying a σ_m^{Me} value of -0.17 . Such an unprecedented low value is chemically unreasonable (see Table 6); e.g., the σ_m value for NMe₂ is -0.16 .^{26b} Further, for TMP to fit the linear trend, the $\sum\sigma$ value for TMP would have to be about -2.64 (Figure 7), involving an apparent σ_o^{Me} value of about $(-2.64 - 4\sigma_p^{\text{Me}})/8$, i.e., -0.26 . Such a value implies that each *o*-Me group of TMP in the Ru(TMP)(RSH)₂ species (R = Me, Et, ⁿPr, ⁱPr, ⁿBu, ^tBu, ⁿHex) is as good an electron donor as a *p*-OMe group (Table 6). Electronic substituent effects alone are clearly unable to explain the different behavior of the Ru(TMP)(RSH)₂ and especially Ru(T-*m,m'*-Me₂PP)(RSH)₂ species; steric effects must play a role.

NMR studies on [Co(T-*o,o'*-X₂PP)(amine)_n]Cl complexes (X = H, F, Cl, Me) have shown that the porphyrin ring current depends on X,⁴⁵ and other theoretical⁴⁶ and experimental⁴⁷ studies on iron and zinc analogues have suggested that this can result qualitatively from the influence of the size of the ortho substituent on the porphyrin π cloud.^{47a} If the *o*-Me groups of the Ru(TMP)(RSH)₂ species behave similarly, a decrease in the ring current could give $\Delta\delta_{\text{SH}}$ values lower than those predicted from purely electronic factors and the trend for the OMe–Cl series. The influence of the meta group in the T-*m,m'*-Me₂PP moiety is less obvious but could be accommodated by the so-called “buttressing effect” or “steric hindrance to resonance”.^{41,48} Although commonly discussed with data from biphenyl and benzoic acid derivatives,^{48a–c} rotational barriers higher than expected upon consideration of the electronic contributions only for meta substituents within *meso*-tetraarylporphyrin complexes have also been reported, including data on ruthenium systems.^{48d} Because aryl ring rotation decreases with the size of the ortho group,⁴⁹ the data suggest that some steric feature of the meta substituents is “sensed” by this group, which is thus perceived by the porphyrin ring as being bigger than it actually is.⁴² Accordingly, the *m*-Me groups of Ru(T-*m,m'*-Me₂PP)(RSH)₂ may indirectly disturb the porphyrin ring current by increasing the apparent radius of the *o*-H atoms. Thus, the different behavior of the Ru(T-*m,m'*-Me₂PP)(RSH)₂ species (versus that of the OMe–Cl series) is similar in nature to that observed for the Ru(TMP)(RSH)₂ complexes, except that the apparent “ortho steric effect” in T-*m,m'*-Me₂PP results from the buttressing effect of the meta substituents, whereas in TMP, the “ortho steric effect” results from a real volume increase in the ortho substituent upon going from T-*p*-XPP to TMP.

The analyses described above for the electronic and steric effects with regard to the Ru(TPP)(RSH)₂ species as reference compounds, with the “absolute” effect of meso substituents on the porphyrin ring current being overlooked. Meso substituents decrease the ring current more than the corresponding β -substituents,^{31a,32d,i} but the electronic effects are insignificant.^{32d} In line with this, $\Delta\delta_{\text{SH}}$ values for Ru(OEP)(RSH)₂ complexes are higher than those of the corresponding *meso*-tetraarylporphyrin species (Table 1). Modeling studies in ruthenium porphyrin systems are limited to a single report by Faller’s group,^{31a} which concluded that the ring current of Ru(mesoporphyrin IX dimethyl ester)(CO)(L), an octa- β -substituted porphyrin species like OEP, is $9 \pm 2\%$ greater than that of Ru(T-*p*-ⁱPrPP)(CO)(L) complexes (L = a nitrogen base). No thiol derivatives were made, but because the σ_p values for *p*-ⁱPr (-0.13) and *p*-Me (-0.14) are similar,^{24,25} a comparison between the Ru(OEP)(RSH)₂ and Ru(T-*p*-

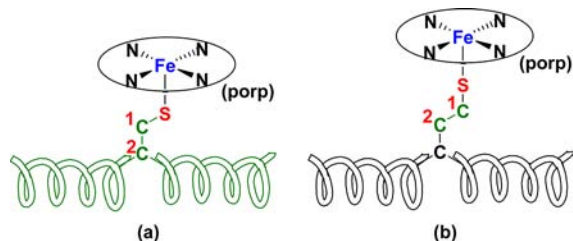
MePP)(RSH)₂ data is reasonable: the $\Delta\delta_{\text{SH}}$ values for the OEP species are higher than those of the T-*p*-MePP species by $10.1 \pm 0.6\%$, remarkable agreement with the $9 \pm 2\%$ value noted above.

4. CONCLUSIONS AND IMPLICATIONS

The findings show that interactions between thiols and ruthenium porphyrins are independent of the electronic properties of the thiol but depend on the bulk volume of groups near the porphyrin plane associated with the steric demands of C¹ and C² of aliphatic thiols; elongation of the alkyl chain beyond C² has no significant effect. These results have intriguing implications for biological systems, particularly within thiolate-heme proteins, most notably the well-studied cytochrome P450,¹⁸ where the role of the proximal thiolate ligand in the unique monooxygenase activity has been demonstrated.^{1c,50} While many studies have focused on delineating the participation of the cysteinate S-Fe bond on O₂ activation and stabilization of high-valent intermediates,^{50a-c,51} Ortiz de Montellano and co-workers^{50c} have focused more on the thiolate role in protein folding, substrate binding, and electron transfer. Other groups have shown^{50d,e} that substrate binding induces a conformational change that leads to the essential low- to high-spin transition in the heme iron, with this being signaled via structural modification of the proximal cysteine.

According to our model for the Ru(porp)(RSH)₂ systems, the sterically relevant C atoms of the cysteine are C^α and C^β (cf. C² and C¹ in Chart 3a), which are associated with V_w^2 and V_w^1 ,

Chart 3. Representation of Thiolate-Bound Heme Proteins: (a) Cysteine; (b) Homocysteine



respectively. Because C^α is directly attached to the protein chain, any conformational change would reflect on the V_w^2 value (as in the BnSH systems) and be readily sensed and acted upon by the heme. Although the mechanistic aspects of P450 are complex, involving a precise orchestration of structural, electronic, and electrostatic features, the short side chain of cysteine likely represents a bonus in the overall process. If homocysteine with an extra C atom was the proximal thiol (Chart 3b), the V_w^{1+2} value for the putative P450 mutant would be associated with two CH₂ groups of the side chain and, therefore, conformational changes in the protein backbone (located in C³) would be more difficult to transmit to the heme group and structural and electronic responses to substrate binding would most likely be compromised. Intriguing, however, is that the biosynthesis of cysteine requires intermediate homocysteine; in effect, nature has evolved a mechanism to deliberately remove one CH₂ group from homocysteine at the expense of using two enzymes and another amino acid, serine.⁵² The biosynthesis of proteins is under tight control, and the incorporation of homocysteine into currently known proteins may contribute to induced pathogenesis.⁵³

There are, of course, differences in the spin states and ionic radii between the metal centers of the Ru(porp)(RSH)₂ and P450-Fe(porp) species, but speculation is considered to be reasonable.

Another related, speculative concept develops if Wächtershäuser's hypotheses that life originated on Fe-S minerals and that primitive biochemical cycles evolved from surface coordination chemistry⁵⁴ are correct. The transition from a surface-supported biocatalyst to a protein-supported enzyme would be less abrupt if the protein could mimic the structural, electronic, and electrostatic features of the mineral surface; as such, the tether between the enzyme prosthetic group and the protein surface should be short, with a preferred use of cysteine versus homocysteine. This implies that nature evolved a biosynthetic pathway to produce cysteine and thus conserve in the new protein-supported enzymes the heterogeneous characteristics of the primitive, surface-supported biocatalyst. Cytochromes P450 are indeed ancient enzymes.⁵⁵ Synthetic chemists, however, when heterogenizing homogeneous catalysts via attachment to a surface or support, preferentially use long tethers in attempts to minimize interference of the support with the solution properties of the catalyst.

The Ru(porp)(RSH)₂ systems provide an entry to help distinguish the steric and electronic effects within ligand coordination onto rigid scaffolds and surfaces and may provide a database for further modeling studies and theoretical calculations of porphyrin π ring currents. Corresponding studies on the mechanism of recognition of primary amines by ruthenium porphyrins, using findings for the thiol systems, have been completed^{13b} and will be reported elsewhere.

■ ASSOCIATED CONTENT

Supporting Information

¹H NMR data for free thiols and correlation analyses of ruthenium porphyrin/thiol interactions. This material is available free of charge via the Internet at <http://pubs.acs.org>.

■ AUTHOR INFORMATION

Corresponding Author

*E-mail: brj@chem.ubc.ca, jsreboucas@quimica.ufpb.br.

Notes

The authors declare no competing financial interest.

■ ACKNOWLEDGMENTS

We thank the Natural Sciences and Engineering Research Council of Canada for financial support and Colonial Metals Inc. for the loan of RuCl₃·xH₂O. J.S.R. acknowledges Fundação CAPES (The Ministry of Education of Brazil) and The University of British Columbia for graduate scholarships.

■ REFERENCES

- (1) For example: (a) Scheidt, W. R.; Reed, C. A. *Chem. Rev.* **1981**, *81*, 543–555. (b) Mayo, S. L.; Ellis, W. R., Jr.; Crutchley, R. J.; Gray, H. B. *Science* **1986**, *233*, 948–952. (c) Dawson, J. H. *Science* **1988**, *240*, 433–439. (d) Moore, G. R.; Pettigrew, G. W. *Cytochromes c: Evolutionary, Structural, and Physicochemical Aspects*; Springer-Verlag: Berlin, 1990; pp 370–372. (e) Sono, M.; Roach, M. P.; Coulter, E. D.; Dawson, J. H. *Chem. Rev.* **1996**, *96*, 2841–2887. (f) Raman, C. S.; Martásek, P.; Masters, B. S. S. In *The Porphyrin Handbook*; Kadish, K. M., Smith, K. M., Guilard, R., Eds.; Academic Press: New York, 2000; Vol. 4, Chapter 34, pp 293–339. (g) Mansuy, D.; Battioni, P. In *The Porphyrin Handbook*; Kadish, K. M., Smith, K. M., Guilard, R., Eds.; Academic Press: New York, 2000; Vol. 4, Chapter 26, pp 1–15.

- (h) Newcomb, M.; Hollenberg, P. F.; Coon, M. J. *Arch. Biochem. Biophys.* **2003**, *409*, 72–79. (i) Guengerich, F. P. *Drug Metab. Rev.* **2004**, *36*, 159–197. (j) Poulos, T. L. *Drug Metab. Dispos.* **2005**, *33*, 10–18. (k) Ortiz de Montellano, P. R. *Drug Metab. Rev.* **2008**, *40*, 405–426. (l) Grigg, J. C.; Ukpabi, G.; Gaudin, C. F. M.; Murphy, M. E. P. *J. Inorg. Biochem.* **2010**, *104*, 341–348. (m) Nielsen, M. J.; Moeller, H. J.; Moestrup, S. K. *Antioxid. Redox Signaling* **2010**, *12*, 261–273. (n) Fasan, R. *ACS Catal.* **2012**, *2*, 647–666.
- (2) For example: (a) James, B. R. In *The Porphyrins*; Dolphin, D., Ed.; Academic Press: New York, 1977; Vol. V, Chapter 6, pp 205–302. (b) Jones, R. D.; Summerville, D. A.; Basolo, F. *Chem. Rev.* **1979**, *79*, 139–179. (c) Traylor, T. G. *Acc. Chem. Res.* **1981**, *14*, 102–109. (d) Suslick, K. S.; Reinert, T. J. *J. Chem. Educ.* **1985**, *62*, 974–983. (e) David, S.; James, B. R.; Dolphin, D.; Traylor, T. G.; Lopez, M. A. *J. Am. Chem. Soc.* **1994**, *116*, 6–14. (f) Collman, J. P.; Boulatov, R.; Sunderland, C. J.; Fu, L. *Chem. Rev.* **2004**, *104*, 561–588.
- (3) For example: (a) Sage, J. T.; Champion, P. M. In *Comprehensive Supramolecular Chemistry*; Suslick, K. S., Ed.; Pergamon: Oxford, U.K., 1996; Vol. 5, Chapter 6, pp 171–218. (b) Hlavica, P.; Schulze, J.; Lewis, D. F. V. *J. Inorg. Biochem.* **2003**, *96*, 279–297. (c) Hlavica, P. *Biochim. Biophys. Acta* **2006**, *1764*, 645–70. (d) Hlavica, P.; Lehnerer, M. *Curr. Drug Metabol.* **2010**, *11*, 85–104. (e) Conner, K. P.; Woods, C. M.; Atkins, W. M. *Arch. Biochem. Biophys.* **2011**, *507*, 56–65. (f) Hlavica, P. *J. Inorg. Biochem.* **2011**, *105*, 1354–1364. (g) Correia, M. A.; Sinclair, P. R.; De Matteis, F. *Drug Metabol. Rev.* **2011**, *43*, 1–26. (h) Otyepka, M.; Berka, K.; Anzenbacher, P. *Curr. Drug Metabol.* **2012**, *13*, 130–142.
- (4) (a) Meunier, B. *Chem. Rev.* **1992**, *92*, 1411–1456. (b) Suslick, K. S.; van Deusen-Jeffries, S. In *Comprehensive Supramolecular Chemistry*; Suslick, K. S., Ed.; Pergamon: Oxford, U.K., 1996; Vol. 5, Chapter 5, pp 141–170. (c) Feiters, M. C.; Rowan, A. E.; Nolte, R. J. M. *Chem. Soc. Rev.* **2000**, *29*, 275–384. (d) Groves, J. T.; Shalyaev, K.; Lee, J. In *The Porphyrin Handbook*; Kadish, K. M., Smith, K. M., Guillard, R., Eds.; Academic Press: New York, 2000; Vol. 4, Chapter 27, pp 17–40. (e) Suslick, K. S. In *The Porphyrin Handbook*; Kadish, K. M., Smith, K. M., Guillard, R., Eds.; Academic Press: New York, 2000; Vol. 4, Chapter 28, pp 41–63. (f) Simonneaux, G.; Le Maux, P. *Coord. Chem. Rev.* **2002**, *228*, 43–60. (g) Ezhova, M. B.; James, B. R. In *Advances in Catalytic Activation of Dioxygen by Metal Complexes*; Simándi, L. I., Ed.; Kluwer Academic Publishers: Dordrecht, The Netherlands, 2003; Chapter 1, pp 1–77.
- (5) (a) Iseki, Y.; Inoue, S. *J. Chem. Soc., Chem. Commun.* **1994**, 2577–2578. (b) Sugimoto, H.; Inoue, S. *Pure Appl. Chem.* **1998**, *70*, 2365–2369. (c) Ogoshi, H.; Mizutani, T. *Curr. Opin. Chem. Biol.* **1999**, *3*, 736–739. (d) Purrello, R.; Gurreri, S.; Lauceri, R. *Coord. Chem. Rev.* **1999**, *190–192*, 683–706. (e) Sugimoto, H.; Kimura, T.; Inoue, S. *J. Am. Chem. Soc.* **1999**, *121*, 2325–2326. (f) Ogoshi, H.; Mizutani, T.; Hayashi, T.; Kuroda, Y. In *The Porphyrin Handbook*; Kadish, K. M., Smith, K. M., Guillard, R., Eds.; Academic Press: New York, 2000; Vol. 6, Chapter 46, pp 279–340. (g) Weiss, J. J. *Inclusion Phenom. Macrocycl. Chem.* **2001**, *40*, 1–22.
- (6) For abbreviations, see the Abstract and Chart 1.
- (7) For example: (a) Imai, H.; Kyuno, E. *Inorg. Chem.* **1990**, *29*, 2416–2422. (b) Imai, H.; Nakagawa, S.; Kyuno, E. *J. Am. Chem. Soc.* **1992**, *114*, 6719–6723. (c) Bonar-Law, R. P.; Sanders, J. K. M. *J. Am. Chem. Soc.* **1995**, *117*, 259–271. (d) Mizutani, T.; Wada, K.; Kitagawa, S. *J. Org. Chem.* **2000**, *65*, 6097–6106. (e) Sen, A.; Suslick, K. S. *J. Am. Chem. Soc.* **2000**, *122*, 11565–11566.
- (8) Bhyrappa, P.; Young, J. K.; Moore, J. S.; Suslick, K. S. *J. Am. Chem. Soc.* **1996**, *118*, 5708–5711.
- (9) Breslow, R.; Yang, J.; Yan, J. *Tetrahedron* **2002**, *58*, 653–659.
- (10) (a) Groves, J. T.; Neumann, R. *J. Am. Chem. Soc.* **1987**, *109*, 5045–5047. (b) Groves, J. T.; Neumann, R. *J. Am. Chem. Soc.* **1989**, *111*, 2900–2909.
- (11) Naruta, Y. In *Metalloporphyrins in Catalytic Oxidations*; Sheldon, R. A., Ed.; Marcel Dekker: New York, 1994; Chapter 8, pp 241–259.
- (12) (a) Kirksey, C. H.; Hambright, P.; Storm, C. *Inorg. Chem.* **1969**, *8*, 2141–2144. (b) Collman, J. P.; Reed, C. A. *J. Am. Chem. Soc.* **1973**, *95*, 2048–2049. (c) Walker, F. A. *J. Am. Chem. Soc.* **1973**, *95*, 1150–1153. (d) Brault, D.; Rougee, M. *Biochem. Biophys. Res. Commun.* **1974**, *57*, 654–656. (e) Abraham, R. J.; Bedford, G. R.; Wright, B. *Org. Magn. Reson.* **1982**, *18*, 45–52. (f) Anzai, K.; Hosokawa, T.; Hatano, K. *Chem. Pharm. Bull.* **1986**, *34*, 1865–1870. (g) Mahmood, A.; Liu, H.; Jones, J. G.; Edwards, J. O.; Sweigart, D. A. *Inorg. Chem.* **1988**, *27*, 2149–2154. (h) Medhi, O. K.; Silver, J. *Inorg. Chim. Acta* **1989**, *166*, 129–133. (i) Zhang, Y.; Jones, J. G.; Sweigart, D. A. *Inorg. Chim. Acta* **1989**, *166*, 85–89.
- (13) (a) Rebouças, J. S.; Patrick, B. O.; James, B. R. *J. Am. Chem. Soc.* **2012**, *134*, 3555–3570. (b) Rebouças, J. S. Ph.D. Dissertation, The University of British Columbia, Vancouver, British Columbia, Canada, 2006.
- (14) (a) Eaton, S. S.; Eaton, G. R. *J. Am. Chem. Soc.* **1975**, *97*, 3660–3666. (b) Rillema, D. P.; Nagle, J. K.; Barringer, L. F., Jr.; Meyer, T. J. *J. Am. Chem. Soc.* **1981**, *103*, 56–62. (c) Barley, M.; Becker, J. Y.; Domazetis, G.; Dolphin, D.; James, B. R. *Can. J. Chem.* **1983**, *61*, 2389–2396. (d) Tavarès, M.; Ramasseul, R.; Marchon, J.-C.; Vallée-Goyet, D.; Gramain, J.-C. *J. Chem. Res. (S)* **1994**, 74–75. (e) Nimri, S.; Keinan, E. *J. Am. Chem. Soc.* **1999**, *121*, 8978–8982.
- (15) Rebouças, J. S.; Cheu, E. L. S.; Ware, C. J.; James, B. R.; Skov, K. A. *Inorg. Chem.* **2008**, *47*, 7894–7907.
- (16) Offord, D. A.; Sachs, S. B.; Ennis, M. S.; Eberspacher, T. A.; Griffin, J. H.; Chidsey, C. E. D.; Collman, J. P. *J. Am. Chem. Soc.* **1998**, *120*, 4478–4487.
- (17) Kuehn, C. G.; Isied, S. S. *Prog. Inorg. Chem.* **1980**, *27*, 153–221.
- (18) (a) Marcus, S. H.; Miller, S. I. *J. Am. Chem. Soc.* **1966**, *88*, 3719–3724. (b) Marciaq-Rousselot, M.-M. *Ann. Chim.* **1971**, *6*, 397–380.
- (19) Chauvel, J. P., Jr.; Folkendt, M. M.; True, N. S. *Magn. Reson. Chem.* **1987**, *25*, 101–104.
- (20) Miller, J. C.; Miller, J. N. In *Statistics for Analytical Chemistry*, 3rd ed.; Ellis Horwood and PTR Prentice Hall: London, 1993; pp 46–50.
- (21) (a) MacPhee, J. A.; Panaye, A.; Dubois, J.-E. *Tetrahedron* **1978**, *34*, 3553–3562. (b) Shorter, J. In *Correlation Analysis of Organic Reactivity, with Particular Reference to Multiple Regression*; Research Studies Press: Chichester, U.K., 1982; Chapter 4, pp 73–126. (c) Gallo, R. *Prog. Phys. Org. Chem.* **1983**, *14*, 115–163. (d) Connors, K. A. In *Chemical Kinetics: The Study of Reaction Rates in Solution*; VCH Publishers: New York, 1990; Chapter 7, pp 311–383.
- (22) Bondi, A. *J. Phys. Chem.* **1964**, *68*, 441–451.
- (23) (a) James, B. R.; Pacheco, A.; Rettig, S. J.; Ibers, J. A. *Inorg. Chem.* **1988**, *27*, 2414–2421. (b) Pacheco, A.; James, B. R.; Rettig, J. A. *Inorg. Chem.* **1999**, *38*, 5579–5587.
- (24) Sjöström, M.; Wold, S. *Chem. Scr.* **1976**, *9*, 200–210.
- (25) Exner, O. In *Correlation Analysis in Chemistry*; Chapman, N. B., Shorter, J., Eds.; Plenum Press: New York, 1978; pp 439–540.
- (26) (a) Reference 21b, pp 27–72. (b) Hansch, C.; Leo, A.; Taft, R. W. *Chem. Rev.* **1991**, *91*, 165–195. (c) Shorter, J. *Pure Appl. Chem.* **1994**, *66*, 2451–2468.
- (27) Brown, H. C.; Stock, L. M. *J. Am. Chem. Soc.* **1962**, *84*, 3298–3306.
- (28) van Bekkum, H.; Verkade, P. E.; Wepster, B. M. *Recl. Trav. Chim. Pays-Bas* **1959**, *78*, 815–850.
- (29) (a) Montgomery, D. C. *Design and Analysis of Experiments*, 3rd ed.; John Wiley & Sons: New York, 1991; pp 521–541. (b) Massart, D. L.; Vandeginste, B. G. M.; Buydens, L. M. C.; de Jong, S.; Lewi, P. J.; Smeyers-Verbeke, J. In *Handbook of Chemometrics and Qualimetrics*; Elsevier: Amsterdam, The Netherlands, 1997; Part A, pp 643–658 and 701–738.
- (30) (a) Walker, F. A.; Hui, E.; Walker, J. M. *J. Am. Chem. Soc.* **1975**, *97*, 2390–2397. (b) Walker, F. A.; Beroiz, D.; Kadish, K. M. *J. Am. Chem. Soc.* **1976**, *98*, 3484–3489. (c) Kadish, K. M.; Bottomley, L. A. *J. Am. Chem. Soc.* **1977**, *99*, 2380–2382.
- (31) (a) Faller, J. W.; Chen, C. C.; Malerich, C. J. *J. Inorg. Biochem.* **1979**, *11*, 151–170. (b) Ball, R. G.; Domazetis, G.; Dolphin, D.; James, B. R.; Trotter, J. *Inorg. Chem.* **1981**, *20*, 1556–1562. (c) Bond, A. D.; Sanders, J. K. M.; Stulz, E. *New J. Chem.* **2011**, *35*, 2691–2696.
- (32) For example: (a) Becker, E. D.; Bradley, R. B. *J. Chem. Phys.* **1959**, *31*, 1413–1414. (b) Ellis, J.; Jackson, A. H.; Kenner, G. W.; Lee, J. *Tetrahedron Lett.* **1960**, *2*, 23–27. (c) Storm, C. B.; Corwin, A. H. J.

- Org. Chem.* **1964**, *29*, 3700–3702. (d) Smith, K. M.; Bobe, F. W.; Minnetian, O. M.; Abraham, R. J. *Tetrahedron* **1984**, *40*, 3263–3272. (e) Arnold, D. P. *J. Chem. Educ.* **1988**, *65*, 1111–1112. (f) Abraham, R. J.; Medforth, C. J. *Magn. Reson. Chem.* **1988**, *26*, 803–812. (g) Cross, K. J.; Crossley, M. J. *Aust. J. Chem.* **1992**, *45*, 991–1004. (h) Kao, Y.-H.; Lecomte, J. T. *J. Am. Chem. Soc.* **1993**, *115*, 9754–9762. (i) Medforth, C. J. In *The Porphyrin Handbook*; Kadish, K. M., Smith, K. M., Guillard, R., Eds.; Academic Press: New York, 2000; Vol. 5, Chapter 35, pp 1–80. (j) Gomes, J. A. N. F.; Mallion, R. B. *Chem. Rev.* **2001**, *101*, 1349–1383. (k) Lecomte, J. T. J.; Vu, B. C.; Falzone, C. J. *J. Inorg. Biochem.* **2005**, *99*, 1585–1592.
- (33) (a) Jusélius, J.; Sundholm, D. *Phys. Chem. Chem. Phys.* **2000**, *2*, 2145–2151. (b) Steiner, E.; Fowler, P. W. *ChemPhysChem* **2002**, *3*, 114–116. (c) Terazono, Y.; Dolphin, D. *J. Org. Chem.* **2003**, *68*, 1892–1900. (d) Steiner, E.; Soncini, A.; Fowler, P. W. *Org. Biomol. Chem.* **2005**, *3*, 4053–4059. (e) Havenith, R. W. A.; Meijer, A. J. H. M.; Irving, B. J.; Fowler, P. W. *Mol. Phys.* **2009**, *107*, 2591–2600. (f) Feixas, F.; Solà, M.; Swart, M. *Can. J. Chem.* **2009**, *87*, 1063–1073. (g) Lash, T. D. *J. Porphyrins Phthalocyanines* **2011**, *15*, 1093–1115.
- (34) Gouterman, M. *J. Chem. Phys.* **1959**, *30*, 1139–1161.
- (35) (a) Antipas, A.; Buchler, A. W.; Gouterman, M.; Smith, P. D. *J. Am. Chem. Soc.* **1978**, *100*, 3015–3024. (b) Barley, M.; Dolphin, D.; James, B. R.; Kirmaier, C.; Holten, D. *J. Am. Chem. Soc.* **1984**, *106*, 3937–3943. (c) Morishima, I.; Takamuki, Y.; Shiro, Y. *J. Am. Chem. Soc.* **1984**, *106*, 7666–7672. (d) Morishima, I.; Shiro, Y.; Nakajima, K. *Biochemistry* **1986**, *25*, 3576–3584. (e) Rachlewicz, K.; Latos-Grażyński, L. *Inorg. Chim. Acta* **1988**, *144*, 213–216.
- (36) (a) Ohya, T.; Sato, M. *Bull. Chem. Soc. Jpn.* **1996**, *69*, 3201–3205. (b) Ikezaki, A.; Ikeue, T.; Nakamura, M. *Inorg. Chim. Acta* **2002**, *335*, 91–99.
- (37) (a) James, B. R.; Sams, J. R.; Tsin, T. B.; Reimer, K. J. *J. Chem. Soc., Chem. Commun.* **1978**, 746–747. (b) Ohya, T.; Morohoshi, H.; Sato, M. *Inorg. Chem.* **1984**, *23*, 1303–1305. (c) Ohya, T.; Sato, M. *J. Chem. Soc., Dalton Trans.* **1996**, 1519–1523.
- (38) Kashiwagi, H.; Obara, S. *Int. J. Quantum Chem.* **1981**, *20*, 843–859.
- (39) (a) Spiro, T. G.; Stong, J. D.; Stein, P. *J. Am. Chem. Soc.* **1979**, *101*, 2648–2655. (b) Helms, J. H.; ter Haar, L. W.; Hatfield, W. E.; Harris, D. L.; Jayaraj, K.; Toney, G. E.; Gold, A.; Mewborn, T. D.; Pemberton, J. R. *Inorg. Chem.* **1986**, *25*, 2334–2337. (c) Kim, D.; Su, Y. O.; Spiro, T. G. *Inorg. Chem.* **1986**, *25*, 3993–3997. (d) Parthasarathi, N.; Hansen, C.; Yamaguchi, S.; Spiro, T. G. *J. Am. Chem. Soc.* **1987**, *109*, 3865–3871. (e) Predergast, K.; Spiro, T. G. *J. Am. Chem. Soc.* **1992**, *114*, 3793–3801. (f) Vitols, S. E.; Roman, J. S.; Ryan, D. E.; Blackwood, M. E., Jr.; Spiro, T. G. *Inorg. Chem.* **1997**, *36*, 764–769.
- (40) Charton, M. *Prog. Phys. Org. Chem.* **1971**, *8*, 235–317.
- (41) (a) Decouzon, M.; Ertk, P.; Exner, O.; Gal, J.-F.; Maria, P.-C. *J. Am. Chem. Soc.* **1993**, *115*, 12071–12078. (b) Kulhánek, J.; Decouzon, M.; Gal, J.-F.; Maria, P.-C.; Fiedler, P.; Jiménez, P.; Roux, M.-V.; Exner, O. *Eur. J. Org. Chem.* **1999**, 1589–1594. (c) Roithová, J.; Exner, O. *J. Phys. Org. Chem.* **2001**, *14*, 752–758.
- (42) Böhm, S.; Fiedler, P.; Exner, O. *New J. Chem.* **2004**, *28*, 67–74.
- (43) (a) Bowden, K.; Grubbs, E. J. *Prog. Phys. Org. Chem.* **1993**, *19*, 183–224. (b) Böhm, S.; Exner, O. *Chem.—Eur. J.* **2000**, *6*, 3391–3398.
- (44) Reference 13b, Chapters 5 and 6.
- (45) Abraham, R. J.; Marsden, I. *Tetrahedron* **1992**, *48*, 7489–7504.
- (46) Vangberg, T.; Ghosh, A. *J. Am. Chem. Soc.* **1998**, *120*, 6227–6230.
- (47) (a) Koerner, R.; Wright, J. L.; Ding, Z. D.; Nasset, M. J. M.; Aubrecht, K.; Watson, R. A.; Barber, R. A.; Mink, L. M.; Tipton, A. R.; Norvell, C. J.; Skidmore, K.; Simonis, U.; Walker, F. A. *Inorg. Chem.* **1998**, *37*, 733–745. (b) Nasset, M. J. M.; Cai, S.; Shokhireva, T. K.; Shokhirev, N. V.; Jacobson, S. E.; Jayaraj, K.; Gold, A.; Walker, F. A. *Inorg. Chem.* **2000**, *39*, 532–540.
- (48) (a) Reiger, M.; Westheimer, F. H. *J. Am. Chem. Soc.* **1950**, *72*, 19–28. (b) Dippy, J. F. J.; Hughes, S. R. C.; Laxton, J. W. *J. Chem. Soc.* **1954**, 1470–1476. (c) Westheimer, F. H. In *Steric Effects in Organic Chemistry*; Newman, M. S., Ed.; John Wiley & Sons: New York, 1956; Chapter 12, pp 523–555. (d) Shroyer, A. L. W.; Lorberau, C.; Eaton, S. S.; Eaton, G. R. *J. Org. Chem.* **1980**, *45*, 4296–4302. (e) Decouzon, M.; Exner, O.; Gal, J.-F.; Maria, P.-C. *J. Chem. Soc., Perkin Trans. 2* **1996**, 475–479.
- (49) (a) Crossley, M. J.; Field, L. D.; Forster, A. J.; Harding, M. H.; Sternhell, S. *J. Am. Chem. Soc.* **1987**, *109*, 341–348. (b) Bott, G.; Field, L. D.; Sternhell, S. *J. Am. Chem. Soc.* **1990**, *102*, 5618–5626.
- (50) (a) Poulos, T. L. *J. Biol. Inorg. Chem.* **1996**, *1*, 356–359. (b) Yoshioka, S.; Takahashi, S.; Ishimori, K.; Morishima, I. *J. Inorg. Biochem.* **2000**, *81*, 141–151. (c) Auclair, K.; Moënne-Loccoz, P.; Ortiz de Montellano, P. R. *J. Am. Chem. Soc.* **2001**, *123*, 4877–4885. (d) Unno, M.; Christian, J. F.; Sjodin, T.; Benson, D. E.; Macdonald, I. D. G.; Sligar, S. G.; Champion, P. M. *J. Biol. Chem.* **2002**, *277*, 2547–2553. (e) Davydov, D. R.; Botchkareva, A. E.; Kumar, S.; He, Y. Q.; Halpert, J. R. *Biochemistry* **2004**, *43*, 6475–6485. (f) Vatsis, K. P.; Peng, H.-M.; Coon, M. J. *Arch. Biochem. Biophys.* **2005**, *434*, 128–138.
- (51) (a) Liu, H. I.; Sono, M.; Kadkhodayan, S.; Hager, L. P.; Hedman, B.; Hodgson, K. O.; Dawson, J. H. *J. Biol. Chem.* **1995**, *270*, 10544–10550. (b) Gross, Z.; Nimri, S.; Barzilay, C. M.; Simkhovich, L. *J. Biol. Inorg. Chem.* **1997**, *2*, 492–506. (c) Ogliaro, F.; de Visser, S. P.; Groves, J. T.; Shaik, S. *Angew. Chem., Int. Ed.* **2001**, *40*, 2874–2878. (d) Tani, F.; Matsu-ura, M.; Nakayama, S.; Naruta, Y. *Coord. Chem. Rev.* **2002**, *226*, 219–226.
- (52) Lehninger, A. L. In *Principles of Biochemistry*; Worth Publishers: New York, 1982; pp173–175 and 618–620.
- (53) Jakubowski, H. *J. Biol. Chem.* **2000**, *275*, 21813–21816.
- (54) (a) Wächtershäuser, G. *Microbiol. Rev.* **1988**, *52*, 452–484. (b) Wächtershäuser, G. *Prog. Biophys. Mol. Biol.* **1992**, *58*, 85–201. (c) Huber, C.; Wächtershäuser, G. *Science* **1997**, *276*, 245–247. (d) Huber, C.; Wächtershäuser, G. *Science* **1998**, *281*, 670–672. (e) Wächtershäuser, G. *Proc. Natl. Acad. Sci. U.S.A.* **1994**, *91*, 4283–4287. (f) Wächtershäuser, G. *Science* **2002**, *298*, 748.
- (55) Danielson, P. D. *Curr. Drug Metab.* **2002**, *3*, 561–597.